mice (*Nf1*^{tm1Fcr}/+)[17] were obtained from the Jackson Laboratory (Bar Harbor, ME, USA). Breeding pairs of C57BL/6 heterozygous P0-deficient mice (*P0*+/–)[18] were provided by Professor Melitta Schachner, University of Hamburg. The genotypes of these animals were determined by PCR analysis using DNA extracted from mouse tails as described in the following section. Primary cultures of dorsal root ganglia (DRG) and adjacent peripheral nerves collected from 9-week-old NPC mice (*npc*^{nih} /*npc*^{nih}, *npc*^{nih}/+), 21–35-week-old P0-deficient mice (*P0*–/–, *P0*+/–) as well as their wild-type littermates (*P0*+/+), and 11-week-old heterozygous *NF1*-deficient mice (*Nf1*^{Fcr}/+) were prepared as described.[10,13,19] Cells were resuspended in feeding medium consisted of 5% FCS (Moregate, Melbourne, Vic., Australia), 50 units/mL penicillin and 50 μg/mL streptomycin in Iscove's modified Dulbecco's minimum essential medium (Invitrogen, Carlsbad, CA, USA), seeded on plastic dishes (Iwaki, Tokyo, Japan) and maintained in 5% CO_2 at 37°C. After repeated treatment with mouse monoclonal antibody to mouse Thy-1.2 and rabbit complement to eliminate fibroblasts,[13,19] the cultures were fed twice a week and passaged once in 4–6 weeks. After 6–8 months in culture, spontaneously emerging colonies were isolated using cloning rings and expanded further. For immunofluorescence and electron microscopy, cells were seeded on poly L-lysine-coated 9-mm ACLAR round coverslips (Allied Fibers and Plastics, Pottsville, PA, USA) at a density of $1–2 \times 10^4$ cells per coverslip. Spontaneously immortalized Schwann cells established from wild-type adult mouse, IMS32,[10] were seeded on dishes and coverslips and maintained in the same medium.

Cytological analysis

For indirect immunofluorescence for S100, laminin, p75^{NTR}, NG2 chondroitin sulfate proteoglycan, and GFAP, cells on coverslips were fixed with 4% paraformaldehyde in PBS and post-fixed with methanol as described.[10] After washings, cells were incubated for 1 h at room temperature with rabbit antibodies to S100 (Dako, Denmark), laminin (Sigma, St Louis, MO, USA), p75^{NTR} (Promega, Madison, WI, USA), NG2 (Chemicon, Temecula, CA, USA), and GFAP (Dako) at dilutions of 1:100. This was followed by incubation for 1 h at room temperature with FITC-conjugated goat antirabbit IgG (Cappel, ICN Pharmaceuticals, Aurora, OH, USA) at a dilution of 1:100. For double labeling of intracellular unesterified cholesterol and GM2 ganglioside, cells on coverslips were fixed in 4% formaldehyde, washed in PBS and incubated in 50 μg/mL filipin (Sigma) in PBS as described.[13] After washing in PBS, cells were incubated with mouse monoclonal antibody to GM2 ganglioside[20] and rhodamine-conjugated goat antimouse IgM (Cappel) as described.[13] To examine the efflux of cationic dye acriflavine from the endosomal/lysosomal compartment, living cells on coverslips were incubated with 10 μg/mL of acriflavine (Sigma), washed thoroughly, incubated in feeding medium and fixed in 4% formaldehyde in PBS as described.[13] Coverslips were mounted on glass slides with 20% glycerol/10% polyvinyl alcohol in 0.1 mol/L Tris-HCl buffer, pH 8.0, and examined under an Olympus AX80TR microscope equipped with ultraviolet, fluorescein and rhodamine optics. For electron microscopic analysis, cells on coverslips were fixed in 1% glutaraldehyde in PBS, post-fixed in 1% osmium tetroxide and processed as described.[13] Ultrathin sections stained with uranyl acetate and lead citrate were examined under a Hitachi H9000 electron microscope.

Polymerase chain reaction

For PCR analysis of *NPC1*, *P0* and *NF1* genes, genomic DNA was isolated from mouse tails and cultured cells using G NOME® (Bio 101, Vista, CA, USA) according to the manufacturer's instruction. Oligonucleotide primers (Invitrogen) were used to amplify sequences containing genome mutations: *NPC1*[21] (mp25–8F, 5′-GGTGCTG GACAGCCAAGT-3′; mp25-INTR3, 5′-GATGGTCTGT TCTCCCATG-3′); *P0*[18] (P0ex1F, 5′-TCTCCATTGCA CATGCCAGGC-3′; P0ex1R, 5′-ACTCAGTGGCTTCA CTTACCC-3′; pMC1neopAF, 5′-TCATCTCACCTTGC TCCTGC-3′; pMC1neopAR, 5′-TATGTCCTGATAGCG GTCCG-3′); *NF1*[17] (NF31a, 5′-GTATTGAATTGAAG CACCTTTGTTTGG-3′; NF31b, 5′-CTGCCCAAGGCT CCCCCAG-3′; NeoTkp, GCGTGTTCGAATTCGCCA ATG-3′). The PCR amplification program consisted of denaturation at 95°C for 1 min, annealing at 60°C for 1 min, and extension at 72°C for 1 min for 35 cycles.

For reverse transcription followed by PCR (RT-PCR), total RNA was isolated from cultured cells using RNAzol™ B (Tel-Test, Friendswood, TX, USA) according to the manufacturer's instruction. First strand cDNA was synthesized from total RNA using random primer and Superscript II reverse transcriptase (Invitrogen). Oligonucleotide primers (Invitrogen) for PCR were designed to amplify cDNA for (i) Schwann cell-associated molecules: S100, p75^{NTR}, L1, P0, peripheral myelin protein-22 (PMP-22), growth associated protein-43 (GAP-43), uridine diphosphate (UDP)-galactose ceramide galactosyltransferase (CGT), and myelin and lymphocyte protein (MAL/MVP17/VIP17); (ii) transcription factors: Pax3, Krox-20 (Egr-2), suppressed cyclic adenosine monophosphate-inducible POU (SCIP; Oct-6/Tst-1), Sox10, mammalian achaete-scute homolog (MASH)1, Egr-1 (Krox-24), c-Jun, cyclic adenosine monophosphate responsive element-

binding protein (CREB), and nuclear factor (NF)κB; and (iii) neurotrophic factors: NGF, BDNF, neurotrophin-3 (NT3), ciliary neurotrophic factor (CNTF), glial cell line-derived neurotrophic factor (GDNF), TGF -β1, -β2 and -β3, and VEGF, as listed in Table 1[22–36] and described elsewhere.[10,13] Primers for RT-PCR of *NPC1* mRNA have also been described.[13] The PCR amplification program consisted of denaturation at 95°C for 1 min, annealing at 55°C for 1.5 min, and extension at 72°C for 1.5 min for 35 cycles. In case of SCIP and MASH1 amplification, PCRx Enhancer Solution (Invitrogen) was added to the reaction mixtures according to the manufacturer's instruction. Samples from non-reverse transcriptase-treated RNA were processed for PCR using the same sets of primers to exclude contaminating genomic DNA as a source of amplified products. The PCR products were subjected to electrophoresis on a 1.5% agarose gel stained with ethidium bromide. To confirm the sequence identity of the amplified products, the PCR fragments were subcloned into pCRII vector (Invitrogen) and sequenced by a model 373A sequencer and the dye terminator cycle sequencing kit (Perkin-Elmer, Foster City, CA, USA).

Western blot analysis

Total cell lysates of confluent Schwann cell cultures were prepared as described,[13] electrophoresed on 4–20% gradient SDS/polyacrylamide gels under reduced conditions and transferred to polyvinyliden diflouride (PVDF) membrane (Atto, Tokyo, Japan). The blotted membrane was blocked with 3% skim milk and incubated overnight with rabbit anti-*NPC1* antibody[37] (1:1000) or rabbit antineurofibromin antibody (NF1GRP (D), 1:200; Santa Cruz), followed by incubations with biotinylated antirabbit IgG (1:1000; Vector, Burlingame, CA, USA) and streptavidin–alkaline phosphatase (1:1,000, Invitrogen). Reac-

Table 1 Primer sequences used for PCR amplification†

Primers	Sequence (position)	Base pairs (bp)	Ref. no. (GenBank accession numbers)
S100	5′-TGGTTGCCCTCATTGATGTC-3′ (23–42)	247	22
	5′-TCAAAGAACTCATGGCAGGC-3′ (269–250)		(NM009115)
CGT	5′-AGTGACGCGTCTTTGGAATA-3′ (280–299)	653	23
	5′-CTCCTACTTCAGCAGGATAC-3′ (933–914)		(X92122)
MAL	5′-ACCTCCCCTGACTTGCTCTT-3′ (99–118)	416	24
	5′-CCCGATDTGCTGTCCTATGA-3′ (514–495)		(Y07626)
Pax-3	5′-AGTGAGCACCTTTGCCAGTA-3′ (12–31)	438	25
	5′-AGAGGCCTGCCGTTGATAAA-3′ (449–430)		(X59358)
Krox-20	5′-TCGAAAGTACCCTAACAGGC-3′ (1202–1221)	471	26
	5′-TCAGCCAGAGCTTCATCTCA-3′ (1672–1663)		(X06746)
SCIP	5′-TCAAGCAACGACGCATCAAG-3′ (1479–1498)	306	27
	5′-GCTTGGGACACTTGAGAAAG-3′ (1784–1765)		(M88302)
Sox10	5′-CATGGCCGAGGAACAAGACCTATC-3′ (53–76)	747	28
	5′-AGCTCTGTCTTTGGGGTGGTTGGA-3′ (799–776)		(AF047043)
MASH1	5′-ATGGAGAGCTCTGGCAAGAT-3′ (76–95)	463	29
	5′-AGCGTCTCCACCTTGCTCAT-3′ (539–520)		(M95603)
Egr-1	5′-GATGCAATTGATGTCTCCGC-3′ (279–298)	741	30
	5′-CAGATAGTCAGGGATCATGG-3′ (1020–1001)		(M20157)
c-Jun	5′-CAATGGGCACATCACCACTA-3′ (866–885)	510	31
	5′-TCCTGAGACTCCATGTCGAT-3′ (1375–1356)		(X12740)
CREB	5′-TTTGACGCGGTGTGTTACGT-3′ (36–55)	541	32
	5′-CCCTGGTGCATCAGAAGATA-3′ (576–557)		(M95106)
NFκB	5′-ACCATGGACGATCTGTTTCC-3′ (58–77)	445	33
	5′-GCTCCTCTATAGGAACGTGA-3′ (502–483)		(M61909)
NGF	5′-GTTGTTCTACACTCTGATCA-3′ (281–300)	497	34
	5′-CACTGTTGTTAATGTTCACC-3′ (777–758)		(K01759)
BDNF	5′-GTGATGACCATCCTTTTCCT-3′ (75–94)	756	35
	5′-CCACTATCTTCCCCTTTTAA-3′ (830–811)		(X55573)
VEGF	5′-ACGCCCTCCGAAACCATGAA-3′ (72–91)	633, 501	36
	5′-TCTGGTTCCCGAAACCCTGA-3′ (704–695)		(M95200)

†Primer sequences for $p75^{NTR}$ (432 bp), L1 (577 bp), P0 (692 bp), peripheral myelin protein-22 (483 bp), growth-associated protein-43 (681 bp), neurotrophin-3 (294 bp), ciliary neurotrophic factor (191 bp), glial cell line-derived neurotrophic factor (641 bp), TGF -β1 (401 bp), -β2 (446 bp) and -β3 (462 bp), and *NPC1* (1294 bp) have been described in previous reports.[10,13]

CGT, uridine diphosphate-galactose ceramide galactosyltransferase; MAL, myelin and lymphocyte protein; SCIP, suppressed cyclic adenosine monophosphate-inducible POU; MASH1, XXXmammalian achaete-scute homolog 1; CREB, cyclic adenosine monophosphate responsive element-binding protein; $^{NF\kappa B}$, nuclear factor $^{\kappa}$B.

tions were visualized by color development using nitroblue tetrazolium/5-bromo-4-chloro-3-indolylphosphate (NBT/BCIP) solution (Roche, Germany).

RESULTS

In the primary cultures of DRG and peripheral nerves derived from wild-type and mutant mice as examined in previous[5,13,14,19] and the present studies, neurons, Schwann cells and fibroblasts were identified by their morphology (Fig. 1a) and by immunocytochemical staining (data not shown). Regardless of origin of animals, these neurons were in every case viable for at least 3 weeks *in vitro*, comparable to those obtained from wild-type DRG and peripheral nerves.[5,13,14,19] When primary cultures were repeatedly treated with antibody to mouse Thy.1.2 and rabbit complement for the first 2–3 weeks *in vitro*, the cultures consisted of >95% of Schwann cells and <5% of fibroblasts (Fig. 1b). These cells were fed twice a week, passaged once in 3 or 4 weeks and maintained for 4–8 months. These cells, designated long-term Schwann cells, retained their spindle-shaped morphology (Fig. 1c) and immunoreactivity for S100, laminin and $p75^{NTR}$ (data not shown), and showed relatively rapid growth as compared to primary Schwann cells. After 6–8 months *in vitro*, spontaneously developed colonies were observed in long-term Schwann cell cultures from all the cases (Fig. 1d). They were separated using the cloning ring, expanded and then batches of cell lines were established from all the animals examined (Table 2). These cell lines were spindle-shaped, were not contact-inhibited and formed ball-shaped subcolonies when the cultures reached confluence.

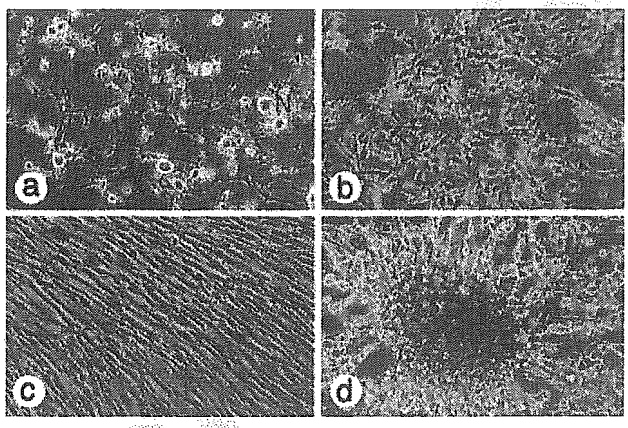

Fig. 1 Phase contrast microscopy of cultures of dorsal root ganglia (DRG) and peripheral nerves derived from 6 week-old wild-type ICR mice. (**a**) Primary cultures containing neurons (N), Schwann cells (S) and fibroblasts (F) at 2 days *in vitro*. (**b**) Short-term cultured Schwann cells at 2 weeks *in vitro* after the treatment of anti-Thy.1.2 and complement. (**c**) Long-term cultured Schwann cells at 2 months *in vitro*. (**d**) Spontaneously developed colony in long-term Schwann cell culture at 6 months *in vitro*.

In the present study one of the formerly established wild-type cell lines, IMS32 (Fig. 2a),[10] was characterized more in detail by immunofluorescence and RT-PCR for sets of Schwann cell-associated molecules, transcription factors, and neurotrophic factors. The IMS32 cells expressed all these phenotypes as examined. The IMS32 cells were intensely immunostained for S100, laminin, $p75^{NTR}$, NG2, and GFAP (Fig. 2b–f). The IMS32 cells also expressed NCAM, L1, GDNF receptor α1 (GFRα1), and erbB2 receptor (neu) as demonstrated by immunofluorescence and Western blot analysis (Watabe *et al.* unpubl. obs., 2002). The mRNA expression of S100, $p75^{NTR}$, L1, P0, PMP-22, GAP-43, CGT, and MAL was confirmed by RT-PCR analysis (Fig. 2g). Furthermore, mRNA for the majority of transcription factors known to be essential for development of Schwann cells and formation of peripheral myelin[38,39] were expressed in IMS32 cells; that is, Pax3, Krox-20, SCIP, Sox10, MASH1, Egr-1, c-Jun, CREB, and NFκB (Fig. 2h). In addition, mRNA for neurotrophic factors, NGF, BDNF, NT3, CNTF, GDNF, TGF-β1, -β2 and -β3, and VEGF, were detected by RT-PCR analysis (Fig. 2i). The expression of NGF, BDNF, GDNF, and TGF-β1, -β2 and -β3 proteins was also confirmed by western blot analysis and ELISA (10 and Watabe *et al.* unpubl. data, 2002).

We then examined immortalized Schwann cell lines established from NPC mice (npc^{nih}/npc^{nih}, $npc^{nih}/+$ Fig. 3), P0-deficient mice (*P0–/–*, *P0+/–*) with their wild-type littermates (*P0+/+* Fig. 4), and *NF1*-deficient mice ($Nf1^{Fcr}/+$ Fig. 5). All these established cell lines showed distinct immunostaining for S100, laminin, $p75^{NTR}$, NG2, and GFAP, and mRNA transcripts for sets of Schwann cell markers, transcription factors, and neurotrophic factors by

Table 2 Immortalized adult mouse Schwann cell lines established at the authors' institutions

Line	Origin	Mouse strain	Ref. no.
MS1	Wild-type	ICR	5
IMS32	Wild-type	ICR	10
SPMS9	*spm/spm*	C57/BLKsJ	13
TwS1	Twitcher	C57/BL6J	14
573C10	npc^{nih}/npc^{nih}	BALB/c	Present study
574C3	$npc^{nih}/+$	BALB/c	Present study
675C20	*P0-/–*	C57/BL6	Present study
576C2	*P0+/–*	C57/BL6	Present study
577C1	*P0+/+*(wild)	C57/BL6	Present study
654C1	$Nf1^{Fcr}/+$	C57/BL6	Present study

All the Schwann cell lines except MS1 (cells transfected by SV40 large T antigen gene) were established by spontaneous immortalization.

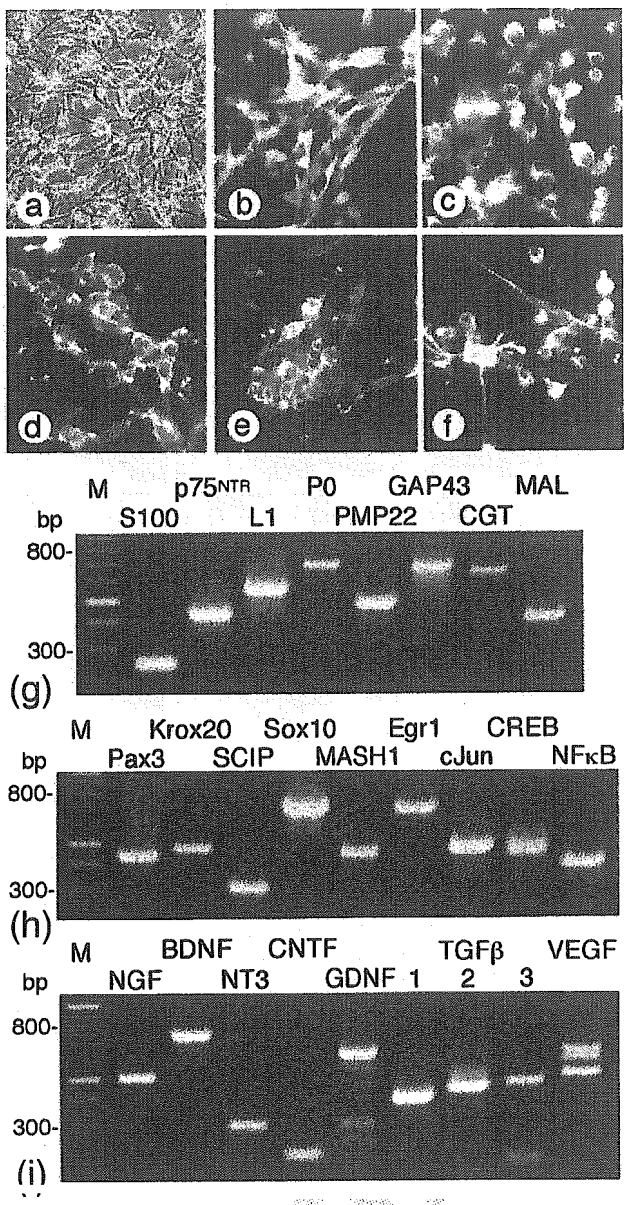

Fig. 2 Phase contrast and immunofluorescence microscopy and RT-PCR analysis of a wild-type IMS32 Schwann cell line. (**a–f**) Phase contrast microscopy (**a**) and immunofluorescence for S100 (**b**), laminin (**c**), p75 ^{NTR} (**d**), NG2 (**e**), and GFAP (**f**). (**g–i**) Expression of mRNA transcripts for Schwann cell-associated molecules (**g**), transcription factors (**h**) and neurotrophic factors (**i**) in IMS32 cells. RT-PCR was performed using primers listed in Table 1. M = 100-bp DNA size markers.

RT-PCR, similar to IMS32 cells as aforementioned (Figs 3–5; Watabe *et al.* unpubl. data, 2002).

The genomic PCR for *NPC1* (a gene responsible for the majority of NPC patients[21,40]) for 573C10 cells established from homozygous npc^{nih}/npc^{nih} mice showed elongated PCR products indicative of genomic deletion of the *NPC1* sequence and insertion of a retrotransposon-like sequence (Fig. 3k).[21] The PCR for the *NPC1* gene of 574C3 cells established from heterozygous $npc^{nih}/+$ mice showed duplicate bands derived from the wild-type and mutated *NPC1* allele,[21] whereas the PCR of SPMS9 (*spm/spm*) cells, for which the exact location of the *NPC1* gene mutation has not yet been identified,[13] gave a single band comparable to that of wild-type IMS32 cells (Fig. 3k). The RT-PCR for *NPC1* showed a marked decrease of *NPC1* mRNA in 573C1 cells as compared to 574C2 cells (Fig. 3j) and wild-type IMS32 cells (not shown), presumably due to nonsense mRNA decay of mutated *NPC1* in 573C10 cells. As expected, *NPC1* protein was not detectable in homozygous 573C10 cell lysates, whereas a distinct 180-kDa band was detected in heterozygous 574C3 cell lysates (Fig. 3l). Like SPMS9 Schwann cells established from *spm/spm* NPC mice[13] and npc^{nih}/npc^{nih} fibroblasts,[16] 573C10 cells showed cytoplasmic granular staining with filipin under a fluorescence microscope using an ultraviolet filter set (Fig. 3e), which indicates intracellular accumulation of unesterified free cholesterol. The 573C10 cells were also intensely immunolabeled with GM2 ganglioside as cytoplasmic granular labeling (Fig. 3f). When we loaded acriflavine for 30 min to 573C10 and 574C3 cells and examined them after 6, 16, and 24 h with a fluorescein filter set, 573C10 cells retained vesicular fluorescence of acriflavine in their cytoplasm after 16 and 24 h (Fig. 3g), whereas 574C3 cells extruded its fluorescence by 16 h after acriflavine loading (not shown), suggesting a defect in the transmembrane efflux pump activity of *NPC1* in the endosomal/lysosomal system of 573C10 cells as well as SPMS9 cells.[13,41] Under the electron microscope, like SPMS9 cells,[13] 573C10 cells exhibited polymorphous inclusions in their cytoplasm (Fig. 3h,i).

As for immortalized Schwann cells established from P0-deficient mice, the genomic PCR analysis for *P0* showed mutated amplified bands in homozygous (*P0–/–*) 675C20 cells and heterozygous (*P0+/–*) 576C2 cells. The P0 mRNA was not detectable in 675C20 cells by RT-PCR analysis (Fig. 4). In a similar manner, we established immortalized Schwann cells from heterozygous *NF1*-deficient mice ($Nf1^{Fcr}/+$). We did not attempt to obtain Schwann cells from homozygous *NF1*-deficient mice ($Nf1^{Fcr}/Nf1^{Fcr}$) in the present study because these animals die in utero resulting from cardiac abnormalities.[17] The 654C1 cells heterozygous for the *NF1* gene exhibited markedly decreased neurofibromin expression as demonstrated by western blot analysis (Fig. 5).

DISCUSSION

We have previously established spontaneously immortalized mouse Schwann cell lines from normal adult mice[10] and, more recently, from murine models of NPC (*spm/*

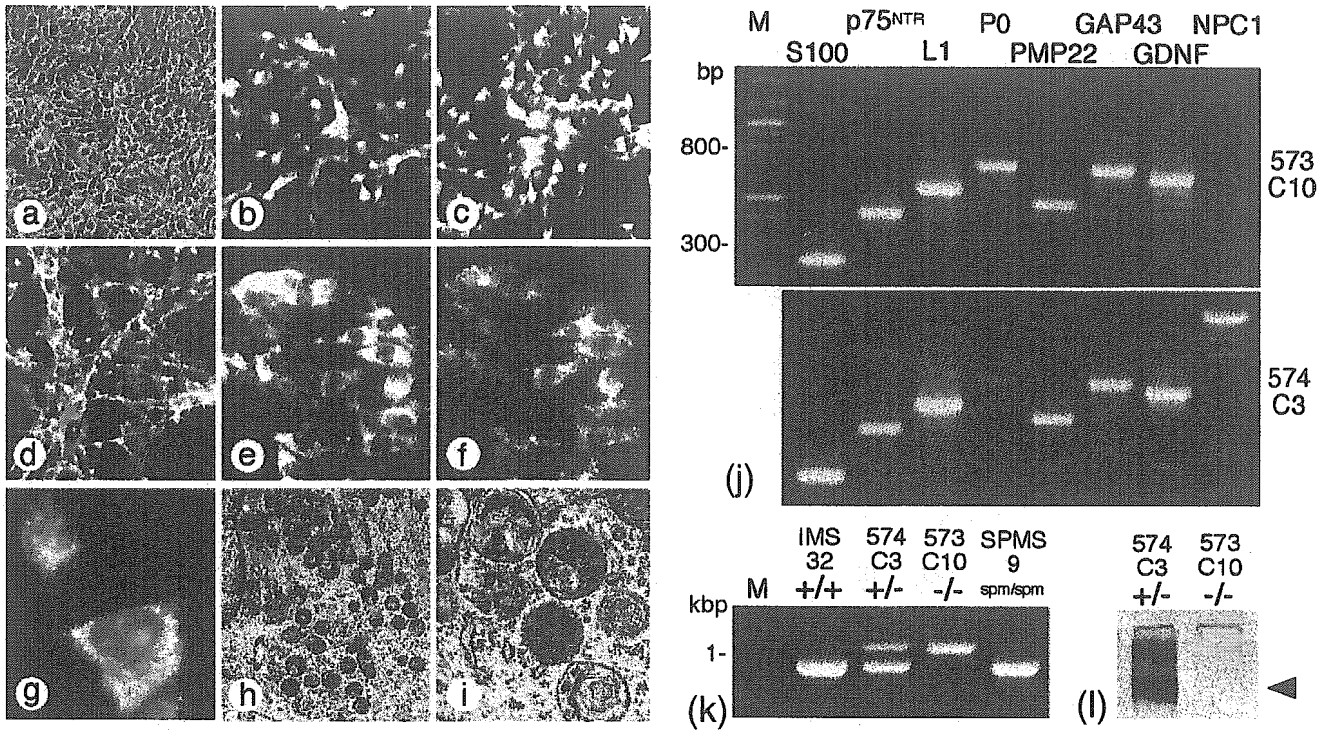

Fig. 3 Phase contrast, fluorescence and electron microscopy, RT-PCR, genomic PCR, and western blot analysis of Schwann cell lines established from Niemann–Pick disease type C (*npc*^{nih}) mice. (**a–d**) Phase contrast microscopy (**a**) and immunofluorescence for S100 (**b**), laminin (**c**) and p75 ^{NTR} (**d**) of 573C10 cells (*npc*^{nih}/*npc*^{nih}). (**a**, ×270; **b–d**, ×400) (**e,f**) Double labeling of cholesterol by filipin (**e**) and GM2 ganglioside by immunofluorescence (**f**) of 573C10 cells. Pictures (**e**) and (**f**) are taken from the same field. (**e,f**, ×500) (**g**) Fluorescence microscopy of 573C10 cells 16 h after acriflavine loading, showing cytoplasmic retention of acriflavine. (**h**) Electron microscopy of a 573C10 cell (×4400). (**i**) Higher magnification showing cytoplasmic inclusions in a 573C10 cell (×19 000). (**j**) RT-PCR analysis of 573C10 (*npc*^{nih}/*npc*^{nih}) and 574C3 (*npc*^{nih}/+) cells using primers listed in Table 1. M = 100-bp DNA size marker. (**k**) Genomic PCR analysis for *NPC1* of wild-type IMS32, 574C3 (*npc*^{nih}/+), 573C10 (*npc*^{nih}/*npc*^{nih}), and SPMS9 (*spm/spm*) cells. The PCR amplification from IMS32 and SPMS9 cells results in 948-bp fragments; from 573C10 cells, 1067-bp fragments; from 574C3 cells, both 948- and 1067-bp fragments. M = 1-kbp DNA size marker. (**l**) Western blot analysis of 574C3 (*npc*^{nih}/+) and 573C10 (*npc*^{nih}/*npc*^{nih}) cell lysates for *NPC1* (arrowhead; approx. 180 kDa). The cell lysates (20-μg proteins) were electrophoresed, blotted and immunostained for *NPC1* as described in the text.

spm)[13] and globoid cell leukodystrophy (twitcher).[14] In the present study we maintained long-term Schwann cell cultures obtained from DRG and peripheral nerves of other NPC mice (*npc*^{nih}/*npc*^{nih}, *npc*^{nih}/+), P0-deficient mice (*P0–/–*, *P0+/–*) with their wild-type littermates (*P0+/+*), and *NF1*-deficient mice (*Nf1*^{Fcr}/+), and established spontaneously immortalized Schwann cell lines from all these animals. Although the detailed mechanism of spontaneous immortalization of these Schwann cells is still unknown, it has been reported that rat Schwann cells can divide indefinitely under the appropriate culture conditions.[42] So far we have been able to obtain immortalized Schwann cell lines from mice of ICR, BALB/c, and C57BL strains (Table 2), and it is likely that the spontaneous immortalization of long-term cultured Schwann cells is a general phenomenon in both normal (wild-type) and mutant mice.

In the present study we further characterized the formerly established wild-type cell line, IMS32,[10] by immunofluorescence and RT-PCR analysis. The IMS32 cells expressed sets of Schwann cell markers, transcription factors crucial for Schwann cell development and peripheral myelin formation, and neurotrophic factors required for the survival of neurons and the maintenance of neuron–Schwann cell interactions.[38,39] Using IMS32 cells we have recently reported that Ras-extracellular-signal-regulated kinase (ERK)-mediated signaling promotes the expression of CNTF in Schwann cells.[43] To date, more than dozen Schwann cell lines have been established, either by transfection of oncogenes such as SV40 large T antigen gene or by spontaneous immortalization.[1–12] The degree of differentiation and phenotypic expression of these Schwann cell lines differ from each other[44] and IMS32 cells seem to be one of the best-characterized Schwann cell lines at present.

Besides Schwann cell lines derived from normal (wild-type) mice, we have established Schwann cell lines pre-

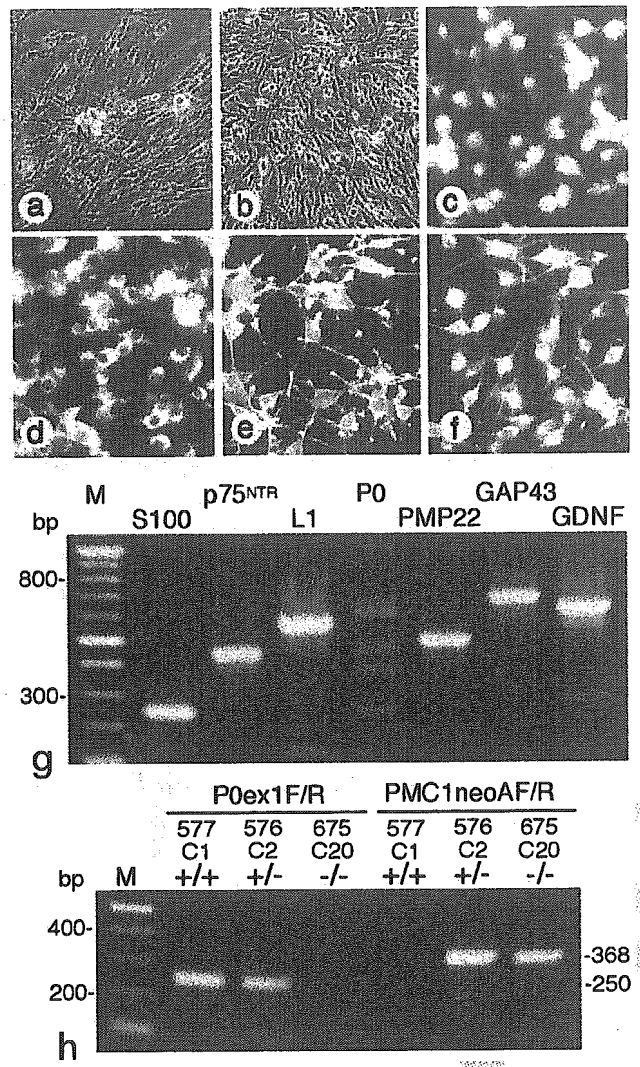

Fig. 4 Phase contrast and immunofluoresence microscopy, RT-PCR, and genomic PCR analysis of Schwann cell lines established from P0-deficient mice. (**a**,**b**) Phase contrast microscopy of *P0–/–* primary culture containing neurons (N) and Schwann cells at 7 days *in vitro* (**a**), and 675C20 *P0–/–* Schwann cell line (**b**). (**c–f**) Immunofluorescence of 675C20 cells for S100 (**c**), laminin (**d**), p75 ^{NTR} (**e**), and GFAP (**f**). (**g**) RT-PCR analysis of 675C20 cells (*P0–/–*) using primers listed in Table 1. M = 100 bp DNA size marker. (**h**) Genomic PCR analysis for *Po* of 577C1 (*P0+/+*), 576C2 (*P0+/–*), and 675C20 (*P0-/–*) cells. Primer pairs P0ex1F/R and PMC1neoAF/R give amplified products corresponding to first coding exon of the *P0* gene (250-bp products) and neo-gene expression cassette inserted into the first exon (368-bp products), respectively. M = 100-bp DNA size marker.

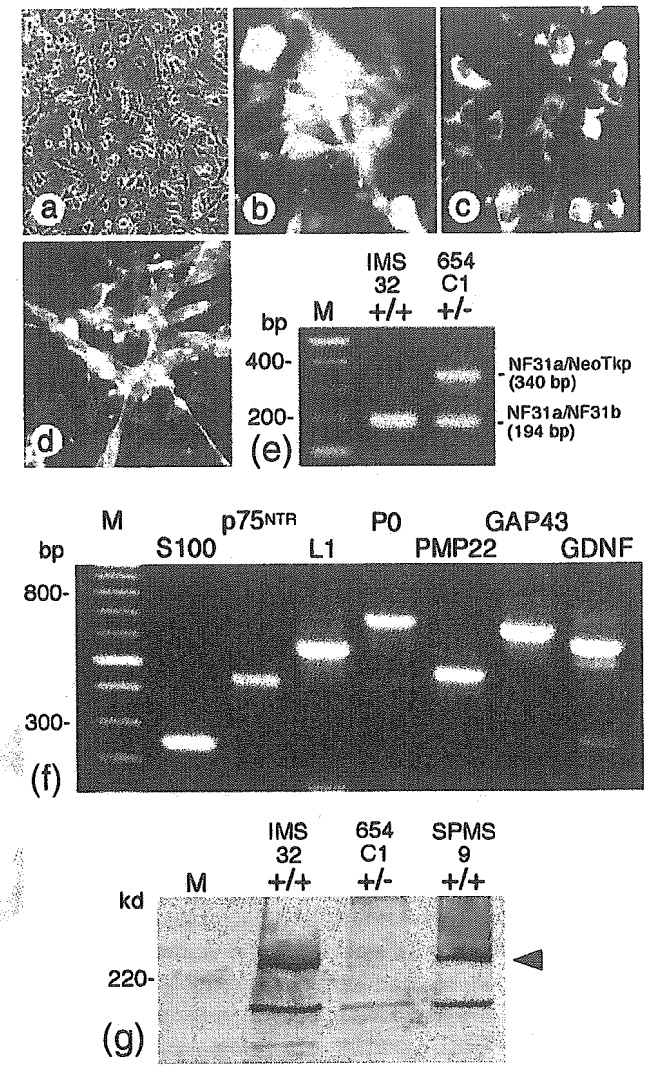

Fig. 5 Phase contrast and immunofluorescence microscopy, genomic PCR, RT-PCR, and western blot analysis of 654C1 Schwann cells established from heterozygous neurofibromatosis type 1 (*NF1*) deficient mice ($Nf1^{Fcr}/+$). (**a–d**) Phase contrast microscopy (**a**) and immunofluorescence for S100 (**b**), laminin (**c**) and p75 ^{NTR} (**d**) of 654C1 cells ($Nf1^{Fcr}/+$). (**e**) Genomic PCR analysis for *NF1* of wild-type IMS32 and 654C1 cells ($Nf1^{Fcr}/+$). The PCR amplification from wild-type cells results in 194-bp fragments; and from heterozygous cells, both 194- and 340-bp fragments.[17] M = 100 bp DNA size marker. (**f**) RT-PCR analysis of 654C1 cells ($Nf1^{Fcr}/+$) using primers listed in Table 1. M = 100-bp DNA size marker. (**g**) Western blot analysis of wild-type IMS32, 654C1 ($Nf1^{Fcr}/+$) and SPMS9 (*spm/spm*) cell lysates for neurofibromin (arrowhead; approx. 250 kDa). The cell lysates (20-μg proteins) were electrophoresed, blotted and immunostained for neurofibromin as described in the text. M = pre-stained molecular weight marker.

viously from *spm/spm* mice (SPMS9 cells)[13] and, in the present study, from BALB/c npc^{nih}/npc^{nih} mice, both of which have been extensively studied as authentic animal models of human NPC.[45–47] Human NPC is an autosomal recessive disorder characterized by the defect of

intracellular transport of cholesterol and the accumulation of unesterified cholesterol in the endosomal/lysosomal system, causing progressive neurodegeneration and death during early childhood.[45–47] The gene responsible for the majority of the disease, *NPC1*, has been cloned,[40] and the discovery of a murine *NPC1* gene has revealed the markedly reduced *NPC1* mRNA in both npc^{nih}/npc^{nih} and *spm/spm* mice.[21] The affected animals develop hepatosplenomegaly and ataxic movements at the age of 7–8 weeks and die by 14 weeks. In the nervous system of npc^{nih}/npc^{nih} and *spm/spm* mice, the most prominent histopathological feature is a marked atrophy of the cerebellum where the loss of Purkinje cells is observed. In addition, neuronal and glial cells containing intracytoplasmic membranous inclusions have been demonstrated in the whole nervous system, accompanied with the degeneration of central and peripheral myelin.[13,47] Like SPMS9 Schwann cells previously established from *spm/spm* mice,[13] 573C10 Schwann cells obtained from npc^{nih}/npc^{nih} mice in the present study had distinct Schwann cell phenotypes and were maintained over 10 months without phenotypic alterations. The genomic PCR of 573C10 cells demonstrated a size alteration in the *NPC1* locus that was identical to that of npc^{nih}/npc^{nih} mouse tissues.[21] The amount of *NPC1* mRNA was markedly decreased, and *NPC1* protein was not detectable in 573C10 cells. These cells were labeled with filipin and intensely immunostained for GM2 ganglioside, confirming their NPC phenotypes. Electron microscopic observation further demonstrated polymorphous inclusions characteristic for NPC in 573C10 cells. It should be noted that cholesterol and sphingolipids including GM2 gangliosides are the main constituents of lipid rafts that function as platforms for transmembrane signaling complexes, and it has been proposed that clinical features associated with NPC can be caused by the accumulation of lipid rafts in the endosomal/lysosomal system.[48] Furthermore, peripheral myelin-related proteins and receptors expresssed by Schwann cells, such as P0, PMP-22, NCAM, MAL, $p75^{NTR}$, GFRα1 and erbB2, are associated with lipid rafts.[49,50] It seems therefore of great importance to investigate whether these raft-associated molecules function or not in NPC1-defective Schwann cells (i.e. SPMS9 cells and 573C10 cells). In addition, like SPMS9 cells,[13] 573C10 cells retained vesicular fluorescence of the cationic dye acriflavine 16–24 h after loading, indicating a defect in the transmembrane efflux pump activity of NPC1 for fatty acids out of the endosomal/lysosomal system in these cells.[41] Taken together, SPMS9 and 573C10 Schwann cell lines can be useful to investigate the pathomechanism of nervous system lesions in NPC, the therapeutic approaches against neurological deficits in patients with NPC, and, more in general, the biology of cholesterol, sphingolipid and fatty acid transports in the nervous system.

In the present study we also established immortalized Schwann cell lines from mice lacking P0 (*P0–/–*, *P0+/–*) due to inactivation of the *P0* gene by homologous recombination and from their wild-type littermates (*P0+/+*).[18] The P0 protein that accounts for more than half of the total PNS myelin protein is expressed by myelinating Schwann cells as components of compact myelin. The P0 protein is a member of the immunoglobulin superfamily of transmembrane proteins that mediates homophilic adhesion in cultured cells and in myelin formation. Most mutations of the *P0* gene are associated with Charcot–Marie–Tooth disease type 1B (CMT1B), a demyelinating peripheral neuropathy in humans.[51,52] The *P0–/–* mice, as used in the present study, are severely hypomyelinated with predominantly uncompacted myelin, are deficient in normal motor coordination, and exhibit tremors and occasional convulsions.[18] Furthermore, the absence of P0 in these animals leads to the dysregulation of myelin gene expression in sciatic nerves such as downregulation of PMP-22 and upregulation of myelin-associated glycoprotein (MAG) and proteolipid protein (PLP), suggesting that P0 is involved in the regulation of both myelin gene expression and myelin morphogenesis.[53] The Schwann cell lines established from these animals in the present study would therefore be useful to investigate the mechanism of complex myelin gene regulation *in vitro*.

NF1, or von Recklinghausen neurofibromatosis, is one of the most common dominant genetic disorders, characterized by the development of multiple benign and malignant nervous system tumors such as neurofibroma, malignant peripheral nerve sheath tumor (MPNST) and glioma.[54] The *NF1* gene, mutated in NF1 disease, encodes neurofibromin that harbors a functional Ras-GTPase-activating protein (GAP) homologous domain and negatively regulates the activation of the Ras intracellular signaling pathway. Cultured Schwann cells obtained from homozygous ($Nf1^{Fcr}/Nf1^{Fcr}$) and heterozygous ($Nf1^{Fcr}/+$) mice demonstrated elevated levels of Ras-GTP, suggesting that neurofibromin is a major Ras-GAP protein in Schwann cells.[55] In the present study we established a 654C1 Schwann cell line from heterozygous ($Nf1^{Fcr}/+$) mice that showed markedly reduced expression of neurofibromin. Our preliminary study showed decreased Ras-GAP activity in 654C1 cells (Araki *et al.* unpubl. obs., 2002). It has recently been shown that, using a conditional knockout strategy, *NF1* LOH in the Schwann cell lineage is sufficient to generate neurofibromas, and *NF1* heterozygosity in the tumor environment promotes neurofibroma formation.[56] Mice with combined mutations in both *NF1* and *p53* genes in *cis* configuration develop MPNST, indicating a role for *p53* mutations in malignant transforma-

tion.[57,58] In addition, *NF1–/–* Schwann cells as well as v-Ras-expressing Schwann cells showed increased expression of P0 protein, suggesting a role for neurofibromin in Schwann cell differentiation via the Ras-signaling pathway.[59] We are currently investigating the regulation of Schwann cell/myelin-related gene and protein expression and its relationship to Ras-GAP activity in heterozygous 654C1 Schwann cells.

In summary, we established spontaneously immortalized Schwann cell lines derived from NPC mice (npc^{nih}/npc^{nih}, npc^{nih}/+), P0-deficient mice (*P0–/–*, *P0+/–*) with their wild-type littermates (*P0+/+*), and NF-1-deficient mice ($Nf1^{Fcr}$/+). Together with previously established wild type,[10] NPC (*spm/spm*),[13] and twitcher[14] Schwann cell lines, these cell lines are considered to be invaluable tools to investigate regulatory mechanisms of Schwann cell growth, neuron–Schwann cell interactions and pathomechanism of nervous system lesions and to explore new therapeutic approaches against neurological deficits in patients with relevant disorders.

ACKNOWLEDGMENTS

We are grateful to Dr Melitta Schachner (University of Hamburg) for providing P0-deficient mice. We thank Dr Tai (Tokyo Metropolitan Institute of Medical Science) for anti-GM2 antibody, Dr William S. Garver (University of Arizona) for anti-*NPC1* antibody, and Dr Kiyomitsu Oyanagi and Emiko Kawakami (Tokyo Metropolitan Institute for Neuroscience) for electron microscopic examination. The present study was supported by Grants-in-Aid for Scientific Research from the Ministry of Education, Science, Sports and Culture of Japan, and Research on Brain Science, Health Sciences Research Grants, the Ministry of Health and Welfare, Japan.

REFERENCES

1. Porter S, Glaser L, Bunge RP. Release of autocrine growth factor by primary and immortalized Schwann cells. *Proc Natl Acad Sci USA* 1987; **84**: 7768–7772.
2. Tennekoon GI, Yoshino J, Peden KWC *et al.* Transfection of neonatal rat Schwann cells with SV-40 large T antigen gene under control of the metallothionein promoter. *J Cell Biol* 1987; **105**: 2315–2325.
3. Chen GL, Halligan NLN, Lue NF, Chen WW. Biosynthesis of myelin-associated proteins in simian virus 40 (SV40)-transformed rat Schwann cell lines. *Brain Res* 1987; **414**: 35–48.
4. Ridley AJ, Paterson HF, Noble M, Land H. Ras-mediated cell cycle arrest is altered by nuclear oncogenes to induce Schwann cell transformation. *EMBO J* 1988; **7**: 1635–1645.
5. Watabe K, Yamada M, Kawamura T, Kim SU. Transfection and stable transformation of adult mouse Schwann cells with SV-40 large T antigen gene. *J Neuropathol Exp Neurol* 1990; **49**: 455–467.
6. Goda S, Hammer J, Kobiler D, Quarles RH. Expression of the myelin-associated glycoprotein in cultures of immortalized Schwann cells. *J Neurochem* 1991; **56**: 1354–1361.
7. Bolin LM, Iismaa TP, Shooter EM. Isolation of activated adult Schwann cells and a spontaneously immortal Schwann cell clone. *J Neurosci Res* 1992; **33**: 231–238.
8. Boutry JM, Hauw JJ, Gansmuller A, Di-Bert N, Pouchelet M, Baron-Van Evercooren A. Establishment and characterization of a mouse Schwann cell line which produces myelin in vivo. *J Neurosci Res* 1992; **32**: 15–26.
9. Toda K, Small JA, Goda S, Quarles RH. Biochemical and cellular properties of three immortalized Schwann cell lines expressing different levels of the myelin-associated glycoprotein. *J Neurochem* 1994; **63**: 1646–1657.
10. Watabe K, Fukuda T, Tanaka J, Honda H, Toyohara K, Sakai O. Spontaneously immortalized adult mouse Schwann cells secrete autocrine and paracrine growth-promoting activities. *J Neurosci Res* 1995; **41**: 279–290.
11. Li R-H, Sliwkowski MX, Lo J, Mather JP. Establishment of Schwann cell lines from normal adult and embryonic rat dorsal root ganglia. *J Neurosci Methods* 1996; **67**: 57–69.
12. Thi AD, Evrard C, Rouget P. Proliferation and differentiation properties of permanent Schwann cell lines immortalized with a temperature-sensitive oncogene. *J Exp Biol* 1998; **201**: 851–860.
13. Watabe K, Ida H, Uehara K *et al.* Establishment and characterization of immortalized Schwann cells from murine model of Niemann–Pick disease type C (spm/spm). *J Periph Nerv Syst* 2001; **6**: 85–94.
14. Shen J-S, Watabe K, Meng XL, Ida H, Ohashi T, Eto Y. Establishment and characterization of spontaneously immortalized Schwann cells from murine model of globoid cell leukodystrophy (Twitcher). *J Neurosci Res* 2002; **68**: 588–594.
15. Pentchev PG, Gal AE, Booth AD *et al.* A lysosomal storage disorder in mice characterized by a dual deficiency of sphingomyelinase and glucocerebrosidase. *Biochim Biophys Acta* 1980; **619**: 669–679.
16. Pentchev PG, Boothe AD, Kruth HS, Weintroub H, Stivers J, Brady RO. A genetic storage disorder in BALB/c mice with a metabolic block in esterification of exogenous cholesterol. *J Biol Chem* 1984; **259**: 5784–5791.
17. Brannan CI, Perkins AS, Vogel KS *et al.* Targeted disruption of the neurofibromatosis type-1 gene leads to

developmental abnormalities in heart and various neural crest-derived tissues. *Genes Dev* 1994; **8**: 1019–1029.
18. Giese KP, Martini R, Lemke G, Soriano P, Schachner M. Mouse P0 gene disruption leads to hypomyelination, abnormal expression of recognition molecules, and degeneration of myelin and axons. *Cell* 1992; **71**: 565–576.
19. Watabe K, Fukuda T, Tanaka J, Toyohara K, Sakai O. Mitogenic effects of platelet-derived growth factor, fibroblast growth factor, transforming growth factor-β, and heparin-binding serum factor for adult mouse Schwann cells. *J Neurosci Res* 1994; **39**: 525–534.
20. Kotani M, Ozawa H, Kawashima I, Ando S, Tai T. Generation of one set of monoclonal antibodies specific for a-pathway ganglio-series gangliosides. *Biochim Biophys Acta* 1992; **1117**: 97–103.
21. Loftus SK, Morris JA, Carstea ED *et al.* Murine model of Niemann–Pick C disease: Mutation in a cholesterol homeostasis gene. *Science* 1997; **277**: 232–235.
22. Jiang H, Shah S, Hilt DC. Organization, sequence, and expression of the murine S100β gene. Transcriptional regulation by cell type-specific cis-acting regulatory elements. *J Biol Chem* 1993; **268**: 20 502–20 511.
23. Bosio A, Binczek E, Stoffel W. Molecular cloning and characterization of the mouse CGT gene encoding UDP-galactose ceramide-galactosyltransferase (cerebroside synthetase). *Genomics* 1996; **35**: 223–226.
24. Magyar JP, Ebensperger C, Schaeren-Wiemers N, Suter U. Myelin and lymphocyte protein (MAL/MVP17/VIP17) and plasmolipin are members of an extended gene family. *Gene* 1997; **189**: 269–275.
25. Goulding MD, Chalepakis G, Deutsch U, Erselius JR, Gruss P. Pax-3, a novel murine DNA binding protein expressed during early neurogenesis. *EMBO J* 1991; **10**: 1135–1147.
26. Chavrier P, Zerial M, Lemaire P, Almendral J, Bravo R, Charnay P. A gene encoding a protein with zinc fingers is activated during G0/G1 transition in cultured cells. *EMBO J* 1988; **7**: 29–35.
27. Hara Y, Rovescalli AC, Kim Y, Nirenberg M. Structure and evolution of four POU domain genes expressed in mouse brain. *Proc Natl Acad Sci USA* 1992; **89**: 3280–3284.
28. Herbarth B, Pingault V, Bondurand N *et al.* Mutation of the Sry-related Sox10 gene in dominant megacolon, a mouse model for human Hirschsprung disease. *Proc Natl Acad Sci USA* 1998; **95**: 5161–5165.
29. Franco del Amo F, Gendron-Maguire M, Gridley T. Cloning, sequencing and expression of the mouse mammalian achaete-scute homolog 1 (MASH1). *Biochim Biophys Acta* 1993; **1171**: 323–327.
30. Sukhatme VP, Cao X, Chang LC *et al.* A zinc finger-encoding gene coregulated with c-fos during growth and differentiation, and after cellular depolarization. *Cell* 1988; **53**: 37–43.
31. Lamph WW, Wamsley P, Sassone-Corsi P, Verma IM. Induction of proto-oncogene JUN/AP-1 by serum and TPA. *Nature* 1988; **334**: 629–631.
32. Ruppert S, Cole TJ, Boshart M, Schmid E, Schutz G. Multiple mRNA isoforms of the transcription activator protein CREB. Generation by alternative splicing and specific expression in primary spermatocytes. *EMBO J* 1992; **11**: 1503–1512.
33. Nolan GP, Ghosh S, Liou HC, Tempst P, Baltimore D. DNA binding and IκB inhibition of the cloned p65 subunit of NF-κB, a rel-related polypeptide. *Cell* 1991; **64**: 961–969.
34. Ullrich A, Gray A, Berman CH, Dull TJ. Human beta-nerve growth factor gene sequence highly homologous to that of mouse. *Nature* 1983; **303**: 821–825.
35. Hofer M, Pagliusi SR, Hohn A, Leibrock J, Barde Y. Regional distribution of brain-derived neurotrophic factor mRNA in the adult mouse brain. *EMBO J* 1990; **9**: 2459–2464.
36. Claffey KP, Wilkison WO, Spiegelman BM. Vascular endothelial growth factor: Regulation by cell differentiation and activated second messenger pathways. *J Biol Chem* 1992; **267**: 16317–16322.
37. Garver WS, Heidenreich RA, Erickson RP, Thomas MA, Wilson JM. Localization of the murine Niemann–Pick C1 protein to two distinct intracellular compartments. *J Lipid Res* 2000; **41**: 673–687.
38. Mirsky R, Jessen KR. The neurobiology of Schwann cells. *Brain Pathol* 1999; **9**: 293–311.
39. Watabe K. Schwann cells. In: Ikuta F (ed.) *Glial Cells.* Tokyo: Kubapuro, 1999; 317–336 (in Japanese).
40. Carstea ED, Morris JA, Coleman KG *et al.* Niemann–Pick C1 disease gene: Homology to mediators of cholesterol homeostasis. *Science* 1997; **277**: 228–231.
41. Davies JP, Chen FW, Ioannou YA. Transmembrane molecular pump activity of Niemann–Pick C1 protein. *Science* 2000; **290**: 2295–2298.
42. Mathon NF, Malcolm DS, Harrisingh MC, Cheng L, Lloyd AC. Lack of replicative senescence in normal rodent glia. *Science* 2001; **291**: 872–875.
43. Abe K, Namikawa K, Honma M *et al.* Inhibition of Ras-extracellular-signal-regulated kinase (ERK) mediated signaling promotes ciliary neurotrophic factor (CNTF) expression in Schwann cells. *J Neurochem* 2001; **77**: 700–703.
44. Hai M, Muja N, DeVries GH, Quarles RH, Patel PI. Comparative analysis of Schwann cell lines as model systems for myelin gene transcription studies. *J Neurosci Res* 2002; **69**: 497–508.
45. Pentchev PG, Vanier MT, Suzuki K, Patterson MC. Niemann–Pick disease type C: A cellular cholesterol

lipidosis. In: Scriver CR, Beaudet AL, Sly WS, Valle D (eds) *The Metabolic and Molecular Bases of Inherited Disease*. New York: McGraw-Hill, 1995; 2625–2640.
46. Liscum L, Klansek JJ. Niemann–Pick disease type C. *Curr Opin Lipidol* 1998; **9**: 131–135.
47. Vanier MT, Suzuki K. Recent advances in elucidating Niemann–Pick C disease. *Brain Pathol* 1998; **8**: 163–174.
48. Simons K, Gruenberg J. Jamming the endosomal system: Lipid rafts and lysosomal storage diseases. *Trends Cell Biol* 2000; **10**: 459–462.
49. Haase B, Bosse F, Müller HW. Proteins of peripheral myelin are associated with glycosphingolipid/cholesterol-enriched membranes. *J Neurosci Res* 2002; **69**: 227–232.
50. Tsui-Pierchala BA, Encinas M, Milbrandt J, Johnson Jr EM. Lipid rafts in neuronal signaling and function. *Trends Neurosci* 2002; **25**: 412–417.
51. Kamholz J, Menichella D, Jani A *et al.* Charcot–Marie–Tooth disease type 1. Molecular pathogenesis to gene therapy. *Brain* 2000; **123**: 222–233.
52. Berger P, Young P, Suter U. Molecular cell biology of Charcot–Marie–Tooth disease. *Neurogenetics* 2002; **4**: 1–15.
53. Xu W, Menichella D, Jiang H *et al.* Absence of P0 leads to the dysregulation of myelin gene expression and myelin morphogenesis. *J Neurosci Res* 2000; **60**: 714–724.
54. Cichowski K, Jacks T. NF1 tumor suppressor gene function: Narrowing the GAP. *Cell* 2001; **104**: 593–604.
55. Kim HA, Rosenbaum T, Marchionni MA, Ratner N, DeClue JE. Schwann cells from neurofibromin deficient mice exhibit activation of $p21^{ras}$, inhibition of cell proliferation and morphological changes. *Oncogene* 1995; **11**: 325–335.
56. Zhu Y, Ghosh P, Charnay P, Burns DK, Parada LF. Neurofibromas in NF1: Schwann cell origin and role of tumor environment. *Science* 2002; **296**: 920–922.
57. Cichowski K, Shih TS, Schmitt E *et al.* Mouse models of tumor development in neurofibromatosis type 1. *Science* 1999; **286**: 2172–2176.
58. Vogel KS, Klesse LJ, Velasco-Miguel S, Meyers K, Rushing EJ, Parada LF. Mouse tumor model for neurofibromatosis type 1. *Science* 1999; **286**: 2176–2179.
59. Rosenbaum T, Kim HA, Boissy YL, Ling B, Ratner N. Neurofibromin, the Neurofibromatosis type 1 Ras-GAP, is required for appropriate P0 expression and myelination. *Ann NY Acad Sci* 1999; **883**: 203–214.

Available online at www.sciencedirect.com
SCIENCE DIRECT®
Neuroscience Research 45 (2003) 219–224
Neuroscience Research
www.elsevier.com/locate/neures

Receptor-type protein tyrosine phosphatase ζ as a component of the signaling receptor complex for midkine-dependent survival of embryonic neurons

Nahoko Sakaguchi [a], Hisako Muramatsu [a], Keiko Ichihara-Tanaka [a], Nobuaki Maeda [b], Masaharu Noda [b], Tokuo Yamamoto [c], Makoto Michikawa [d], Shinya Ikematsu [e], Sadatoshi Sakuma [e], Takashi Muramatsu [a,*]

[a] *Department of Biochemistry, Nagoya University School of Medicine, 65 Tsurumai-cho, Showa-ku, Nagoya 466-8550, Japan*
[b] *Division of Molecular Neurobiology, National Institute for Basic Biology, 38 Nishigonaka, Myodaiji-cho, Okazaki 444-8585, Japan*
[c] *Tohoku University Gene Research Center, Sendai 981, Japan*
[d] *Department of Dementia Research, National Institute for Longevity Sciences, 36-3 Gengo, Morioka, Obu, Aichi, Japan*
[e] *Pharmaceauticals Development Department, Meiji Milk Products Co. Ltd., 540 Naruda, Odawara 250-0862, Japan*

Received 13 August 2002; accepted 29 October 2002

Abstract

Midkine (MK), a heparin-binding growth factor, suppresses apoptosis of embryonic neurons in culture, induced by serum deprivation. Receptor-type protein tyrosine phosphatase ζ (PTP ζ) is a chondroitin sulfate proteoglycan with a transmembrane domain and intracellular tyrosine phosphatase domains. The activity of MK was abolished by digestion with chondroitinase ABC, or addition of the antibody to PTP ζ, while digestion with heparitinase showed no significant effect. These results suggested that the survival-promoting signal of MK was received by a receptor complex containing PTP ζ. Low density lipoprotein receptor-related protein (LRP) has been identified as another component of the signaling receptor. Ectodomains of two related proteins expressed on neurons, namely LRP6 and apoE receptor 2, were FLAG-tagged and examined for MK binding, using MK-agarose column. Both the ectodomains were found to exhibit calcium-dependent binding to MK. These proteins may participate in MK signaling in certain cases. The survival-promoting activity of MK was abolished by PP1, an inhibitor of src protein kinase, pertussis toxin, an inhibitor of G protein-linked signaling and sodium orthovanadate, an inhibitor of PTPs.

Keywords: Apoptosis; Chondroitin sulfate proteoglycan; Low density lipoprotein receptor-related protein; LRP6; Midkine; Receptor-type protein tyrosine phosphatase ζ

1. Introduction

Midkine (MK) is a 13 kDa heparin-binding growth factor with various activities (Kadomatsu et al., 1988; Muramatsu, 2002). It shows anti-apoptotic effects on embryonic neurons in culture (Owada et al., 1999) and on hippocampal neurons exposed to ischemic shock (Yoshida et al., 2001) and also enhances neurite outgrowth and migration of neurons (Kaneda et al., 1996; Maeda et al., 1999; Muramatsu et al., 1993). The signaling receptors of MK have only been partially clarified. In the case of enhancement of migration of embryonic neurons, the receptor-type protein tyrosine phosphatase ζ (PTP ζ)/RPTP β which is a chondroitin sulfate proteoglycan, has been identified as a receptor (Maeda et al., 1999; Maeda and Noda, 1998). PTP ζ is strongly expressed in the brain (Maeda et al., 1994), and has a single transmembrane domain, two tyrosine phosphatase domains and an extracellular domain with an N-terminal carbonic anhydrase-like domain, a fibronectin type III domain, and a large cysteine-free, serine and glycine-rich domain (Krueger and Saito, 1992). On the other hand, in the case of the anti-

* Corresponding author. Tel.: +81-52-744-2059; fax: +81-52-744-2065
E-mail address: tmurama@med.nagoya-u.ac.jp (T. Muramatsu).

0168-0102/02/$ - see front matter
PII: S0168-0102(02)00226-2

apoptotic activity of MK on embryonic neurons, low density lipoprotein receptor-related protein (LRP) has been identified as a component of the signaling receptor (Muramatsu et al., 2000).

Although the migration-enhancing activity and anti-apoptotic activity were both determined using embryonic neurons as target cells, the amounts of MK used and the method of delivery were entirely different; in the anti-apoptotic assay, soluble MK was added at 10–100 ng/ml (Owada et al., 1999), while in the migration-promoting assay, MK at a concentration of 30–70 μg/ml was used to coat the membrane of the assay chamber (Maeda et al., 1999). Thus, it remains possible that different molecules are involved in signal reception. One of the aims of the present investigation was to determine whether PTP ζ is involved in signaling of the anti-apoptotic activity. We also analyzed whether other members of the LDL receptor family, in particular LRP6 and apoE receptor 2 (apoER2) bind to MK, since LRP6 has been found to be a receptor of Wnt (Pinson et al., 2000; Tamai et al., 2000; Wehrli et al., 2000) and Dickkopf (Mao et al., 2001), and apoER2 was shown to be a receptor of reelin (D'Arcangelo et al., 1999; Hiesberger et al., 1999; Trommsdoff et al., 1999). Furthermore, we used inhibitors of signal transduction to gain insight into the initial stage of the intracellular signaling pathway.

2. Materials and methods

2.1. Midkine

Recombinant human MK was expressed in yeast (*Pichia pastoris* GS115) and was purified to homogeneity. MK-agarose was prepared by coupling 40 mg of MK to 8 ml of CNBr-activated Sepharose 4B (Amersham Biosciences.K.K, NJ, USA) as described previously (Muramatsu et al., 2000).

2.2. Determination of anti-apoptotic activity of MK to embryonic neurons

Neural cells were prepared from the cerebral cortex of embryonic day-17 ICR mice as described previously (Owada et al., 1999). Mice were handled according to the guide line set by Nagoya University School of Medicine. The cells were suspended in Dulbecco's-modified Eagle's medium (DMEM)/10% fetal calf serum (FCS), and plated onto poly-D-lysine-coated plastic coverslips (13 mm in diameter, Thermanox, Nalge Nunc International, IL) in 24-well plates at 1×10^5 cells/cm^2. The cells were incubated overnight, washed three times, and cultured for 24 h in DMEM under serum-free conditions with or without 100 ng/ml of chemically synthesized human MK (Peptide Institute, Osaka, Japan). The percentage of apoptotic cells was determined by the TUNEL method using terminal deoxynucleotidyl transferase and biotin-16-2′-deoxyuridine-5′-triphosphate (Gavrieli et al., 1992). The number of TUNEL-positive cells was counted, and the ratio of this cell number to the total cell number was calculated. Without addition of MK, usually 50% of cells were TUNEL-positive. Statistical significance was evaluated by paired *t*-test. The following materials were added to the assay; chondroitinase ABC (protease-free, Seikagaku Kogyo Co., Tokyo, Japan), heparitinase (Seikagaku Kogyo Co.), anti-6B4 proteoglycan (affinity-purified rabbit antibody against the extracellular domain of PTP ζ, Maeda et al., 1994), sodium orthovanadate (Wako, Tokyo, Japan). PP1 (4-amino-5-(4-methylphenyl)-7-(*t*-butyl) pyrazolo [3,4-D] pyrimidine) (Alexis Biochemicals, San Diego, CA), and Pertussis toxin (PTX)(Sigma, St. Louis, MO).

2.3. Binding of FLAG-tagged LRP6 ectodomain to MK

Total RNA was isolated from the cerebral cortex of embroynic day-17 ICR mice using Isogen (Wako Pure Chemical Industries, Ltd., Osaka, Japan). Approximately 5 μg of total RNA was transcribed into single-stranded cDNA using the SUPERSCRIPT™. Preamplification System for the first stand cDNA synthesis (GIBCO BRL, Gaithersburg, MD). FLAG-tagged LRP6 ectodomain (nucleotides 86-4202) was amplified by RT-PCR, and ligated into the pcDNA3.1 vector (Invitrogen Life Technologies, CH Grtonngen, Netherlands). Approximately 4 μg of the DNA was transfected into COS7 cells using LIPOFECTAMINE PLUS Reagent (GIBCO BRL). The transfected cells were cultured in DMEM with 10 % FCS for 24 h and were homogenized in 20 mM Tris–HCl buffer, pH 7.5, containing 1% Triton X-100, 0.15 M NaCl, 1 mM phenylmethylsulfonyl fluoride (PMSF) and 5 μg/ml aprotinin and leupeptin. Cell lysate was applied to 0.5 ml of MK-agarose equilibrated with the above buffer containing 1 mM $CaCl_2$ and $MgCl_2$. The column was eluted with 2.5 ml of the buffer containing increasing concentration of NaCl with 20 mM EDTA and without divalent cations. The elution was also performed without EDTA; in this occasion the buffer used lacked divalent cations. The eluate was subjected to SDS-PAGE, and proteins were transferred onto a nitrocellulose membrane. The membrane was blocked with 5% nonfat milk in PBS containing 0.1% Tween 20 and blotted with anti-FLAG monoclonal antibody (Sigma) and then incubated with HRP-conjugated goat anti-mouse IgG (Jackson ImmunoResearch Laboratories, West Grove, PA). Signals were visualized by ECL detection kit (Amersham Biosciences).

2.4. Binding of FLAG-tagged ApoER2 ectodomain to MK

Experiments were performed as described in Section 2.3. A cDNA encoding the extracellular domain (nucleotide number 94-2574) of apoER2 (Kim et al., 1996) was ligated into pCDNA3.1 with the FLAG-tag sequence. The transfected COS7 cells were cultured for 24 h in DMEM with 10% FCS, washed with PBS and then cultured for 24 h with DMEM without FCS. The culture supernatant collected was made upto 1 mM with respect to PMSF. The buffer used for affinity chromatography lacked 1% Triton X-100 and when indicated contained divalent cations.

3. Results

3.1. Involvement of PTP ζ in mediation of anti-apoptotic activity of MK

To examine the role of PTP ζ in MK-induced suppression of apoptosis of embryonic neurons caused by serum deprivation, we tested two reagents that should interfere with the action of PTP ζ. Chondroitinase ABC, which cleaves chondroitin sulfate chains from proteoglycans including PTP ζ, abolished the action of MK, while heparitinase, which acts on haparan sulfate, showed no significant effect (Fig. 1). Boiled chondroitinase ABC showed no effects. Anti-6B4 proteoglycan, the polyclonal antibody to the extracellular domain of PTP ζ, also abolished the action of MK (Fig. 2). Control IgG showed no effects. These results taken together suggested that PTP ζ is a signaling receptor involved in mediating the anti-apoptotic activity of MK.

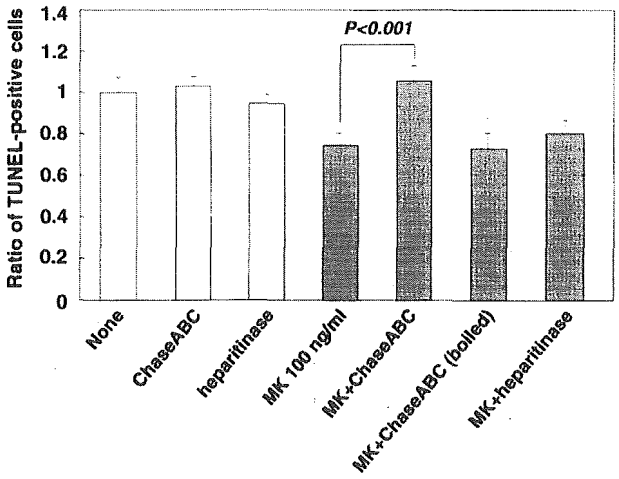

Fig. 1. Chondroitinase digestion of embryonic neurons abolished survival-promoting activity of MK. At 24 h after plating of embryonic neuronal cells, culture medium was changed to serum-free DMEM with or without 30 mU/ml of chondroitinase ABC (Chase ABC). After 1 h incubation, serum-free DMEM with or without 100 ng/ml of MK was added. After 24 h incubation, the ratio of TUNEL-positive cells to total cells was determined, and the results were expressed as ratio to the value obtained without addition of reagents (None). Data are means ±SEM($n = 4$). Three independent experiments showed similar results. $P < 0.001$ versus MK and MK+chondroitinase ABC.

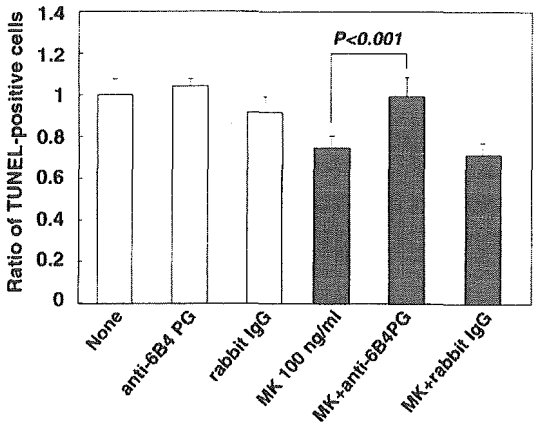

Fig. 2. Effects of affinity-purified antibody against 6B4 proteoglycan on the survival-promoting activity of MK. Anti-6B4 proteoglycan (300 μg/ml) was added 1 h before the addition of MK (100 ng/ml). Data are means ±SEM ($n = 4$). Three independent experiments showed similar results. $P < 0.001$ versus MK and MK+anti-6B4 proteoglycan.

3.2. Binding of ectodomains of LRP6 and apoER2 to MK

FLAG-tagged ectodomains of LRP6 and apoER2 were applied to an MK-agarase column to examine their affinity to MK. Both proteins bound to the column at a NaCl concentration of 0.15 M. In the presence of 20 mM EDTA, most of the LRP6 ectodomain was eluted by 0.2 M NaCl (Fig. 3A, lane 2). By elution without EDTA, the ectodomain was mainly eluted by 0.3 M NaCl, but significant portion was also eluted by 0.4 and 0.5 M NaCl (Fig. 3A, lanes 8–10). Therefore, the binding was calcium-dependent.

Although LRP6 bound to the column after washing with the buffer with 0.15 M NaCl and without divalent cations (Fig. 3A, lane 6), a part of apoER2 was eluted from the column simply by washing with the buffer lacking divalent cations (Fig. 3B, lane 2). Therefore, for elution without EDTA, we used the buffer with divalent cations (Fig. 3B, lanes 8–11). When elution without EDTA and with divalent cations (Fig. 3B, lanes 8–11) was compared with that with EDTA (Fig. 3B, lanes 3–7 and 12), the latter methods attained more efficient elution of apoER2. Therefore, the binding of apoER2 ectodomain to MK was also calcium-dependent.

3.3. Effects of PP1, PTX and vanadate on the anti-apoptotic activity of MK

GITI/Cat-1(Kawachi et al., 2001) and β-catenin (Meng et al., 2000) have been identified as components

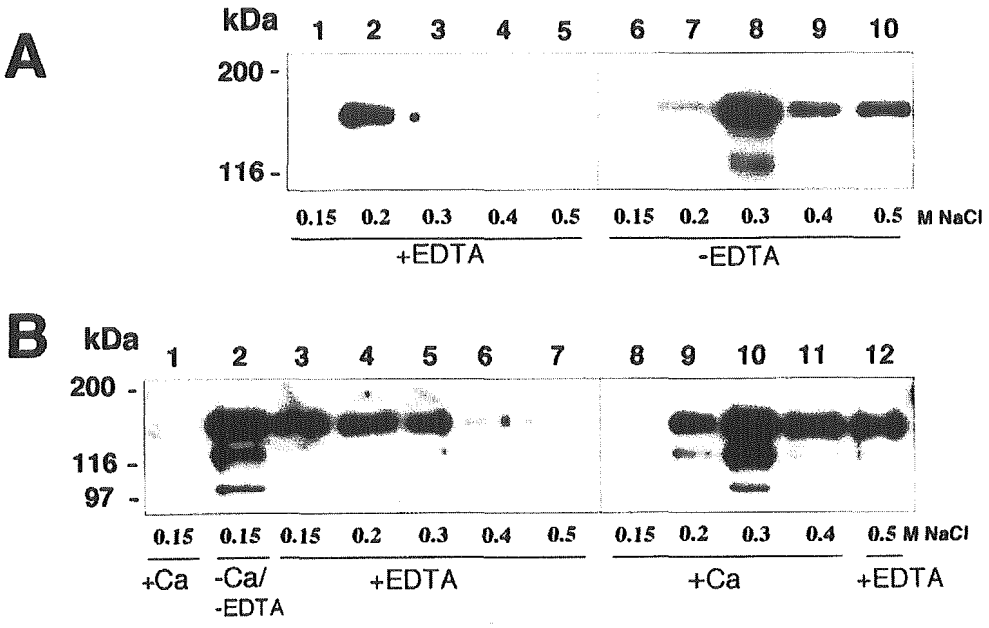

Fig. 3. Binding of FLAG-tagged ectodomains of LRP6 and apoER2 to MK-Sepharose. Experiments were carried out as described in Section 2. Fractions eluted from MK-Sepharose by the indicated NaCl concentrations were subjected to SDS-PAGE in a 7% gel, and analyzed by Western blotting to detect FLAG-tagged proteins. No bands were detected in the unabsorbed fraction. (A) LRP6: Lanes 1–5, elution with the buffer containing 20 mM EDTA; Lanes 6–10, elution with the buffer containing no EDTA. Lanes 1, 6, washate (0.15 M NaCl); 2,7, 0.2 M NaCl; 3, 8, 0.3 M NaCl; 4, 9, 0.4 M NaCl; 5, 10, 0.5 M NaCl. (B) ApoER2: Lanes 1, 8–11, elution with the buffer containing divalent cations; Lane 2, elution with the buffer without divalent cations; Lanes 3–7, 12, elution with 20 mM EDTA. Lanes 1, 2, 3, 8, 0.15 M NaCl; 4, 9, 0.2 M NaCl; 5, 10, 0.3 M NaCl; 6, 11, 0.4 M NaCl; 7, 12, 0.5 M NaCl.

of the signaling system downstream from PTP ζ, and in the present assay system, the importance of PI3 kinase and MAP kinase has been shown (Owada et al., 1999). To gain further insight into the signaling system, we tested three inhibitors, sodium orthovanadate, an inhibitor of PTPs (Huyer et al., 1997), PP1, an inhibitor of src protein kinase (Hanke et al., 1996), and PTX, an inhibitor of G protein-linked signaling (Tsai et al., 1984). All of these reagents strongly inhibited the action of MK, and alone did not promote apoptosis significantly above the control levels (Figs. 4–6).

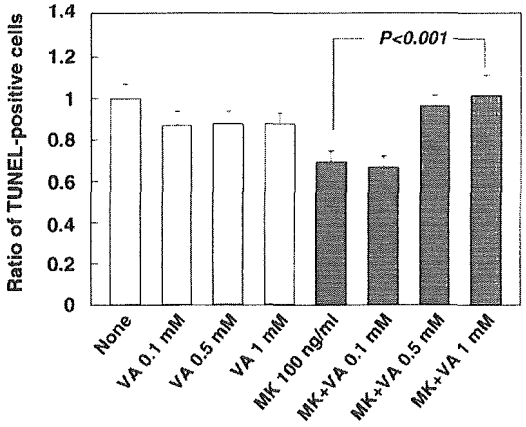

Fig. 4. Effects of phosphatase inhibitor on survival-promoting activity of MK. Sodium orthovanadate (VA : 0.1–1 mM) was added 1 h before the addition of MK (100 ng/ml). Data are means ±SEM ($n = 4$). Three independent experiments showed similar results. $P < 0.001$ versus MK and MK+1 mM sodium orthovanadate (MK–VA 1 mM).

4. Discussion

The present results suggested that PTP ζ is involved in reception of anti-apoptotic signal of MK. The role of PTP ζ in signaling of neuronal migration caused by substratum-bound MK as well as by its family member pleiotrophin (PTN)/heparin-binding growth-associated molecule is well established (Maeda et al., 1999; Maeda and Noda, 1998). PTP ζ is also involved in MK-dependent migration of osteoblastic cells (Qi et al., 2001). The present results extended the role of PTP ζ in signaling of soluble MK.

We previously identified LRP, which is composed of 500 and 85 kDa polypeptides and belongs to the LDL receptor family (Muramatsu et al., 2000; Hiesberger et al., 1999; Trommsdoff et al., 1999), as another component of the signaling receptor. Simultaneously, other members of the LDL receptor family, apoER2 and LRP6, were found as components of reelin receptor (D'Arcangelo et al., 1999) and Wnt and Dickkopf receptor (Bafico et al., 2001; Mao et al., 2001; Pinson et al., 2000; Tamai et al., 2000; Wehrli et al., 2000), respectively. Therefore, we examined whether LRP6 and

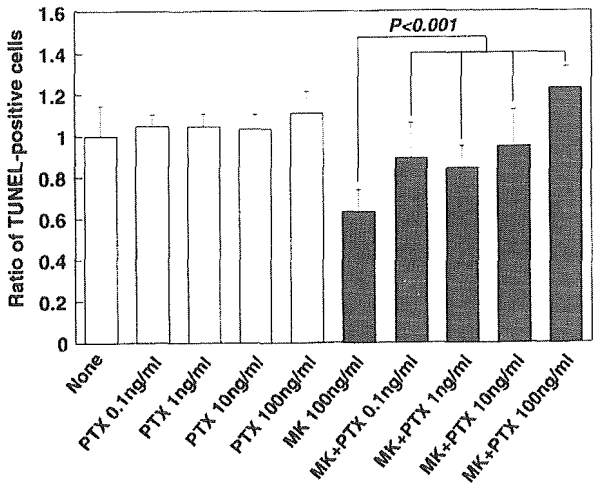

Fig. 5. Effects of PP1 on MK-dependent survival of embryonic neurons. Experiments were performed as described in the legend of Fig. 4.

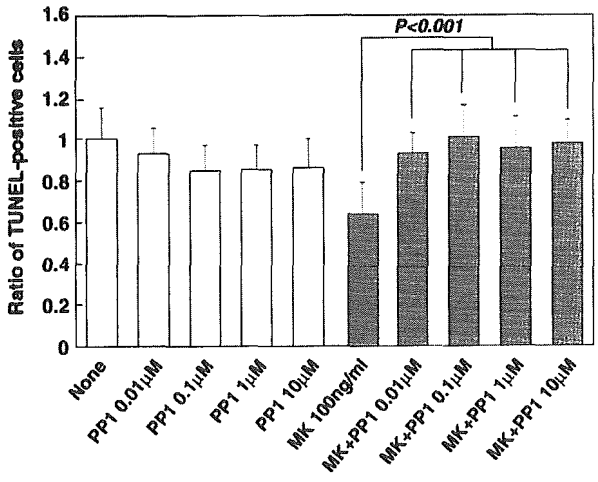

Fig. 6. Effects of PTX on MK-dependent survival of embryonic neurons. Experiments were performed as described in the legend of Fig. 4.

apoER2 bind to MK; our results indicated that both in fact bind to MK. The binding of these ectodomains was calcium-dependent. Although as compared to binding to LRP (Muramatsu et al., 2000), the binding affinities of these ectodomains appeared to be slightly less strong, we should keep in mind the possibility that LRP6 and apoER2 also participate in reception of MK signal. Especially interesting is LRP6, since the difference in cytoplasmic domains of LRP and LRP6 enables the usage of different signaling systems (Brown et al., 1998).

Recently, LRP has been found to be involved in calcium mobilization, and a G protein-linked signaling has been shown to be involved (Bacskai et al., 2000). In the present investigation, we found that MK-dependent survival of embryonic neurons was inhibited by PTX, an inhibitor of G protein-linked signaling (Tsai et al., 1984). PTX was previously found to inhibit MK-induced mobilization of intracellular calcium in neutrophils (Takada et al., 1997). It is possible that PTX inhibits the LRP-associated action of a G protein. PTX can also inhibit the downstream signaling of PTP ζ, since GIT1/Cat-1 (G protein-coupled receptor kinase-interactor1/Cool associated, tyrosine-phosphorylated 1) has been identified as a substrate of PTP ζ (Kawachi et al., 2001).

The inhibition of MK action by vanadate, an inhibitor of PTP cannot be interpreted simply. It is thought that ligand binding leads to downregulation of PTP ζ (Kawachi et al., 2001; Meng et al., 2000). In the presence of vanadate, this signaling process of PTP ζ would be stopped, in addition to the other protein-tyrosine phosphatase.

PP1, a specific inhibitor of src protein kinase (Hanke et al., 1996), also inhibited the anti-apoptotic activity of MK. PP1 also inhibits MK-induced migration of osteoblasts (Qi et al., 2001) and MK-dependent adhesion of oligodendrocyte precursor cells (Rambsby et al., 2000). The downstream signaling system of MK has been identified as PI3 kinase followed by MAP kinase both in the present system (Owada et al., 1999) and promotion of osteoblast migration (Qi et al., 2001). Since src is often located upstream of PI3 kinase (Lee and States, 2000; Versteeg et al., 2000), it is possible that the MK signal received by the receptor complex containing LRP and PTP ζ is transmitted to PI3 kinase via src protein kinase.

Acknowledgements

This work was supported by grants from the Ministry of Education, Science, Sports, Culture and Technology of Japan, Japan Society for the Promotion of Science and from CREST.

References

Bacskai, B.J., Xia, M.Q., Strickland, D.K., Rebeck, G.W., Hyman, B.T., 2000. The endocytosis receptor protein LRP also mediate neuronal calcium signaling via *N*-methyl-D-aspartate receptors. Proc. Natl. Acad. Sci. USA 97, 11551–11556.

Bafico, A., Liu, G., Yanif, A., Gazit, A., Aaronson, S.A., 2001. Novel mechanism of Wnt signaling inhibition mediated by Dickkopf-1 interaction with LRP6/Arrow. Nat. Cell Biol. 3, 683–686.

Brown, S.D., Twells, R.C., Hey, P.J., Cox, R.D., Levy, E.R., Soderman, A.R., Metzker, M.L., Caskey, C.T., Todd, J.A., Hess, J.F., 1998. Isolation and characterization of LRP6, a novel member of the low density lipoprotein receptor gene family. Biochem. Biophys. Res. Commun. 248, 879–888.

D'Arcangelo, G., Homayouni, R., Keshvara, L., Rice, D.S., Sheldon, M., Curran, T., 1999. Reelin is a ligand for lipoprotein receptors. Neuron 24, 471–479.

Gavrieli, Y., Sherman, Y., Ben-Sasoon, S.A., 1992. Identification of programmed cell death in situ via specific labeling of nuclear DNA fragmentation. J. Cell Biol. 119, 493–501.

Hanke, J.H., Gardner, J.P., Dow, R.L., Changerlian, P.S., Brissette, W.H., Weringer, E.J., Pollok, B.A., Connelly, P.A., 1996. Discovery of a novel potent and Src family-selective tyrosine kinase inhibitor. J. Biol. Chem. 271, 695–701.

Hiesberger, T., Trommsdorff, M., Howell, B.W., Goffinet, A., Mumby, M.C., Cooper, J.A., Herz, J., 1999. Direct binding of reelin to VLDL receptor and apoE receptor 2 induces tyrosine phophorylation of disabled-1 and modulates phosphorylation. Neuron 24, 481–489.

Huyer, G., Liu, S., Kelly, J., Moffat, J., Payette, P., Kennedy, B., Tsaprailis, G., Gresser, M.J., Ramachandran, C., 1997. Mechanism of inhibition of protein-tyrosine phosphatases by vanadate and pervanadate. J. Biol. Chem. 272, 843–851.

Kadomatsu, K., Tomomura, M., Muramatsu, T., 1988. cDNA cloning and sequencing of a new gene intensely expressed in early differentiation stages of embryonal carcinoma cells and in midgestation period of mouse embryogenesis. Biochem. Biophys. Res. Commun. 151, 1312–1318.

Kaneda, N., Talukder, A.H., Nishiyama, H., Koizumi, S., Muramatsu, T., 1996. Midkine, a heparin-binding growth/differentiation factor, exhibits nerve cell adhesion and guidance activity for neurite outgrowth in vitro. J. Biochem. 119, 1150–1156.

Kawachi, H., Fujikawa, A., Maeda, N., Noda, M., 2001. Identification of GIT1/Cat-1 as a substrate molecule of protein tyrosine phosphatase ζ/β by the yeast substrate-trapping system. Proc. Natl. Acad. Sci. USA 98, 6593–6598.

Kim, D.H., Iijima, H., Goto, K., Sakai, J., Ishii, H., Kim, H.J., Suzuki, H., Kondo, S., Saeki, S., Yamamoto, T., 1996. Human apolipoprotein E receptor 2. A novel lipoprotein receptor of the low density lipoprotein receptor family predominantly expressed in brain. J. Biol. Chem. 271, 8373–8380.

Krueger, N.X., Saito, H., 1992. A human transmembrane protein-tyrosine-phosphatase, PTP ζ, is expressed in brain and has an N-terminal receptor domain homologous to carbonic anhydrases. Proc. Natl. Acad. Sci. USA 89, 7417–7421.

Lee, A.W., States, D.J., 2000. Both src-dependent and -independent mechanisms mediate phosphatidylinositol 3-kinase regulation of colony-stimulating factor-1 activated mitogen-activated protein kinases in myeloid progenitors. Mol. Cell Biol. 20, 6779–6798.

Maeda, N., Hamanaka, H., Shintani, T., Nishiwaki, T., Noda, M., 1994. Multiple receptor-like protein tyrosine phosphatases in the form of chondroitin sulfate proteoglycan. FEBS Lett. 354, 67–70.

Maeda, N., Ichihara-Tanaka, K., Kimura, T., Kadomatsu, K., Muramatsu, T., Noda, M., 1999. A receptor-like protein-tyrosine phosphatase PTP ζ/RPTP β binds a heparin-binding growth factor midkine. Involvement of arginine 78 of midkine in the high affinity binding to PTP ζ. J. Biol. Chem. 274, 12474–12479.

Maeda, N., Noda, M., 1998. Involvement of receptor-like protein tyrosine phosphatase PTP ζ/RPTP β and its ligand pleiotrophin/heparin-binding growth-associated molecule (HB-GAM) in neuronal migration. J. Cell Biol. 142, 203–216.

Mao, B., Wu, W., Li, Y., Hoppe, D., Stannek, P., Glinka, A., Niehrs, C., 2001. LDL-receptor-related protein 6 is a receptor for Dickkopf proteins. Nature 411, 321–325.

Meng, K., Rodriguez-Peña, A., Dimitriv, T., Chen, W., Yamin, M., Noda, M., Deuel, T.F., 2000. Pleiotrophin signals increased tyrosine phosphorylation of β-catenin through inactivation of the intrinsic catalytic activity of the receptor-type protein tyrosine phsophatase β/ζ. Proc. Natl. Acad. Sci. USA 97, 2603–2608.

Muramatsu, H., Shirahama, H., Yonezawa, S., Maruta, H., Muramatsu, T., 1993. Midkine, a retinoic acid-inducible growth/differentiation factor: immunochemical evidence for the function and distribution. Dev. Biol. 159, 392–402.

Muramatsu, H., Zou, K., Sakaguchi, N., Ikematsu, S., Sakuma, S., Muramatsu, T., 2000. LDL receptor-related protein as a component of the midkine receptor. Biochem. Biophys. Res. Commun. 270, 936–941.

Muramatsu, T., 2002. Midkine In Wiley Encyclopedia Mol. Med. Wiley, New York, USA, pp. 2086–2088.

Owada, K., Sanjo, N., Kobayashi, T., Mizusawa, H., Muramatsu, H., Muramatsu, T., Michikawa, M., 1999. Midkine inhibitis caspase-dependent apoptosis via the activation of mitogen-activated protein kinase and phosphatidylinositol 3-kinase in cultured neurons. J. Neurochem. 73, 2084–2092.

Pinson, K.I., Brennan, J., Monkley, S., Avery, B.J., Skarnes, W.C., 2000. An LDL-receptor-related protein mediates Wnt signalling in mice. Nature 407, 535–538.

Qi, M., Ikematsu, S., Maeda, N., Ichihara-Tanaka, K., Sakuma, S., Noda, M., Muramatsu, T., Kadomatsu, K., 2001. Haptotactic migration induced by midkine: involvement of protein-tyrosine phosphatase ζ, mitogen-activated protein kinase and phosphatidylinositol 3-kinase. J. Biol. Chem. 276, 15868–15875.

Rambsby, M., Ichihara-Tanaka, K., Kimura, T., Scott, M., Haynes, L., 2000. Bipolar undifferentiated CG-4 oligodendroglial line cells adhere, extend processes and disperse on midkine, a heparin-binding growth factor: orthovanadate and chondroitin sulfate E inhibit cell attachment. Neurosci. Res. Commun. 28, 31–39.

Takada, T., Kinkori, T., Muramatsu, H., Hayakawa, A., Torii, S., Muramatsu, T., 1997. Midkine, a retinoic acid-inducible heparin-binding cytokine, is a novel regulator of intracellular calcium in human neutrophils. Biochem. Biophys. Res. Commun. 241, 756–761.

Tamai, K., Semenov, M., Kato, Y., Spokony, R., Liu, C., Katsuyama, Y., Hess, F., Saint-Jeannet, J.P., He, X., 2000. LDL-receptor-related proteins in Wnt signal transduction. Nature 407, 530–535.

Trommsdoff, M., Gotthardt, M., Hiesberger, T., Shelton, J., Stockinger, W., Nimpf, J., Hammer, R.E., Richerdson, J.A., Herz, J., 1999. Reeler/Disabled-like disruption of neuronal migration in knockout mice lacking the VLDL receptor and apoE receptor 2. Cell 97, 689–701.

Tsai, S.C., Adamik, R., Kannaho, Y., Hewlett, E.L., Moss, J., 1984. Effects of guanyl nucleotides and rhodopsin on ADP-ribosylation of the inhibitory GTP-binding component of adenylate cyclase by pertussis toxin. J. Biol. Chem. 259, 15320–15323.

Versteeg, H.H., Hoedemaeker, I., Diks, S.H., Stam, J.C., Spaargaren, M., van Bergen En Henegouwen, P.M., van Deventer, S.J., Peppelenbosch, M.P., 2000. Factor VIIa/tissue factor-induced signaling via activation of Src-like kinases, phosphatidylinositol 3-kinase, and Rac. J. Biol. Chem. 275, 28750–28756.

Wehrli, M., Dougan, S.T., Caldwell, K., O'Keefe, L., Schwartz, S., Vaizel-Ohayon, D., Schejter, E., Tomlinson, A., DiNardo, S., 2000. Arrow encodes an LDL-receptor-related protein essential for Wingless signaling. Nature 407, 527–530.

Yoshida, Y., Ikematsu, S., Moritoyo, T., Goto, M., Tsutsui, J., Sakuma, S., Osame, M., Muramatsu, T., 2001. Intraventricular administration of the neurotrophic factor midkine ameliorates hippocampal delayed neuronal death following transient forebrain ischemia in gerbils. Brain Res. 894, 46–55.

Journal of Neuroscience Research 72:141–146 (2003)

Mini-Review

Cholesterol Paradox: Is High Total or Low HDL Cholesterol Level a Risk for Alzheimer's Disease?

Makoto Michikawa*
Department of Dementia Research, National Institute for Longevity Sciences, Aichi, Japan

Cholesterol is an essential component of membranes for maintaining their structure and functions. The discovery that possession of apolipoprotein E (apoE), allele ε4 is a strong risk factor for Alzheimer's disease (AD) leads us to focus on the role of cholesterol in the pathogenesis of AD. Accumulating epidemiological and biological evidence suggests the link between the serum cholesterol level and the development of AD, and the potential therapeutic effectiveness of statins for AD and mild cognitive impairment (MCI), whereas other lines of evidence show controversial results. Cholesterol is known to interact with amyloid β-protein (Aβ) in a reciprocal manner: cellular cholesterol levels modulate Aβ generation, whereas Aβ alters cholesterol dynamics in neurons, leading to tauopathy. In this review, the relationship between the cholesterol levels in serum or cerebrospinal fluid (CSF) and the induction of AD is discussed. The mechanism(s), if this is the case, of how cholesterol in the central nervous system (CNS) is involved in the induction of pathologies of AD including Aβ generation and tauopathy, and how statins prevent it are also discussed.

Key words: Alzheimer's disease; cholesterol; HDL; statin; amyloid cascade; amyloid β-protein; apolipoprotein E

Studies of lipid metabolism have been focusing on that in the systemic circulation using non-neuronal cells for decades; however, knowledge regarding cholesterol metabolism in the central nervous system (CNS), the most lipid-rich organs, is very limited. The cholesterol metabolism in the CNS is postulated to be regulated independently and uniquely, because CNS is segregated from systemic circulation by the blood–brain barrier. The cholesterol transported in the systemic circulation by serum lipoprotein cannot be available to the CNS. Furthermore, the morphology of neurons is quite different from that of other cells, in that neurons have many long, complicated processes, which have an area of membrane that is 10- to 100-fold that of the cell body (Craig and Banker, 1994). More than 20% of clusters of postsynaptic density turn over within 24 hr in the hippocampal neurons (Okabe et al., 1999). These findings suggest that, in addition to cholesterol transportation from the cell body to nerve terminals, local metabolic processing of cholesterol at the nerve terminal must play a critical role in the development and maintenance of neuronal plasticity and functions. In accordance with this notion, it has been shown that cholesterol supplied as a lipoprotein complex, i.e., high-density lipoprotein (HDL), is critical for the maturation of synapses and the maintenance of synaptic plasticity (Koudinov and Koudinova, 2001; Mauch et al., 2001).

ELEVATED SERUM TOTAL AND LOW-DENSITY LIPOPROTEIN CHOLESTEROL LEVELS ARE A RISK FOR ALZHEIMER'S DISEASE

There are increasing bodies of evidence showing that the pathophysiology of Alzheimer's disease (AD) is linked closely to cholesterol metabolism. Recent epidemiological studies have revealed the plausibility of a link between AD and cholesterol metabolism based on an association of an elevated serum total cholesterol level with a risk for the development of AD and mild cognitive impairment (MCI) (Notkola et al., 1998; Kivipelto et al., 2001). Recent findings that cholesterol levels in membranes modulate the association of Aβ with GM1 ganglioside (Kakio et al., 2001, 2002; Yanagisawa and Matsuzaki, 2002), which is thought to be involved in the aggregation of soluble Aβ in AD brain (Yanagisawa et al., 1995), also suggest a link

Contract grant sponsor: Comprehensive Research on Aging and Health, Ministry of Health, Labor, and Welfare, Japan; Contract grant sponsor: Program for Promotion of Fundamental Studies in Health Sciences of the Organization for Pharmaceutical Safety and Research of Japan.

*Correspondence to: Makoto Michikawa, MD, Department of Dementia Research, National Institute for Longevity Sciences, 36-3 Gengo, Morioka, Obu, Aichi 474-8522, Japan. E-mail: michi@nils.go.jp

Received 3 January 2003; Accepted 6 January 2003

Published online 25 February 2003 in Wiley InterScience (www.interscience.wiley.com). DOI: 10.1002/jnr.10585

between AD and cholesterol. The mechanism through which a high serum cholesterol level results in the development of AD remains to be elucidated. This relationship, however, correlates well with the finding that the possession of the apoE allele ε4 is a strong risk factor for AD development, because there is a stepwise increase, as a function of alleles (ε2 to ε3 to ε4), in serum total and low-density lipoprotein (LDL) cholesterol levels (Bouthillier et al., 1983; Davignon et al., 1988; Lehtinen et al., 1995; Braeckman et al., 1996; Frikke-Schmidt et al., 2000). The observation that statin treatment decreases the prevalence of AD (Wolozin et al., 2000) seems to strengthen this notion, because it implies that decreased levels of serum total cholesterol and LDL-cholesterol might lead to a reduced cellular cholesterol level in the CNS, which in turn inhibits the synthesis of amyloid β-protein (Aβ) in neurons (Simons et al., 1998) and secretion of Aβ from cells into the cerebrospinal fluid (CSF) (Fassbender et al., 2001). A recent study has shown that the use of lipid-lowering agents other than statins is also associated with a lower risk for AD in individuals less than 80 years old (Rockwood et al., 2002). These observations raise the hopes that a medicine already in common use may become a "novel" drug for prevention and treatment of MCI and AD.

RELATIONSHIP BETWEEN SERUM AND CSF CHOLESTEROL LEVELS

These data, however, must be interpreted with caution. There seems to be several issues that need to be answered before the idea that high serum cholesterol levels and thus high cholesterol levels in CNS cells are responsible for the development of AD can be accepted fully. Recent studies have shown that there is no significant correlation between CSF cholesterol levels (cholesterol in the CSF exists as an HDL complex) and serum total (or LDL) cholesterol levels (Fagan et al., 2000; Fassbender et al., 2002). It was also shown that the serum cholesterol levels have no effect on the level of HMG-CoA reductase mRNA and its activity in brains (Jurevics et al., 2000). These lines of evidence cannot explain why, in terms of the difference in CNS cholesterol metabolism, significantly higher levels of serum total cholesterol lead to a higher prevalence of AD. With respect to the inhibitory effect of statin on the development of AD, the membrane cholesterol was shown to play a critical role in amyloid β-protein (Aβ) generation by modulating secretase activity (Simons et al., 1998; Kojro et al., 2001). Consistent with these results, the levels of Aβ decreased in the CSF or brains of animals treated with a high dose of statins (Fassbender et al., 2001; Petanceska et al., 2002). It also was shown that diet-induced hypercholesterolemia in animals resulted in significantly increased levels of brain Aβ (Sparks et al., 1994; Sparks, 1996; Refolo et al., 2000), and that a cholesterol-lowering drug ameliorates the Aβ pathology with a positive correlation between the level of serum cholesterol and Aβ accumulation in a transgenic mouse model of AD (Refolo et al., 2001). A recent study, however, has revealed that even though statins at therapeutically relevant doses interfere with CNS cholesterol metabolism and reduce the cholesterol level by inhibiting cholesterol synthesis, at these doses statins do not alter intrathecal secretion of Aβ in patients (Fassbender et al., 2002). This suggests that statins in the therapeutic dose range may prevent development of AD by modulating in a way other than inhibiting Aβ generation. This inconsistency may arise from the difference in the species used, transgenic model mouse and human, the higher doses of statins used for animals than the clinically relevant doses, and the higher levels of cholesterol in the diet used for animals than in the diet used for humans. These results indicate that we should evaluate further the effect of statin treatment at relevant doses on MCI and AD biomarkers by carrying out prospective, randomized, placebo-controlled trials, and also elucidate the mechanism, if any, of underlying statin actions.

ALTERNATIVE INTERPRETATION OF RESULTS LINKING PLASMA HDL CHOLESTEROL WITH A RISK FOR AD

If levels of serum total and LDL cholesterol have no effect on the cholesterol level in the CSF, does it mean that cholesterol in the CNS is not involved in the pathogenesis of AD? With respect to this, another possible interpretation of previous data is proposed. The major concern with previous reports is that the relationship between serum cholesterol levels and AD or MCI were discussed, and HDL cholesterol levels were not focused on (Jarvik et al., 1995; Notkola et al., 1998; Evans et al., 2000; Kivipelto et al., 2001). As described above, the order of the LDL and total cholesterol levels in the serum with respect to the apoE genotypes is apoE2 < apoE3 < apoE4 (Bouthillier et al., 1983; Davignon et al., 1988; Lehtinen et al., 1995; Braeckman et al., 1996; Frikke-Schmidt et al., 2000). When one notes the HDL cholesterol levels in the serum, however, as has been shown in these same reports, they are in the opposite order: apoE2 > apoE3 > apoE4 (Lehtinen et al., 1995; Braeckman et al., 1996; Frikke-Schmidt et al., 2000), which can be explained by the isoform-dependent apoE ability to release cholesterol from cells to generate HDL particles (Michikawa et al., 2000; Gong et al., 2002b). This apoE isoform-dependent HDL cholesterol level is found also in AD patients in whom the serum HDL cholesterol level is correlated inversely with the dose of the apoE allele ε4 (Hoshino et al., 2002). Although CSF lipids remain to be analyzed completely, one study has shown that the level of HDL cholesterol in the serum of AD patients is lower than that of controls and the decreased level is correlated with the severity of AD (Merched et al., 2000). Thus, it is reasonable to conclude the opposite relationship between cholesterol levels and the risk for AD; that is, a low serum HDL cholesterol level is a risk for AD development. Importantly, one should note that the cerebrospinal fluid contains only HDL but not LDL or very low density lipoprotein (VLDL) (Roheim et al., 1979; Pitas et al., 1987a,b; Borghini et al., 1995). It has been reported that the HDL cholesterol level is lower in the CSF of AD patients than in the CSF of

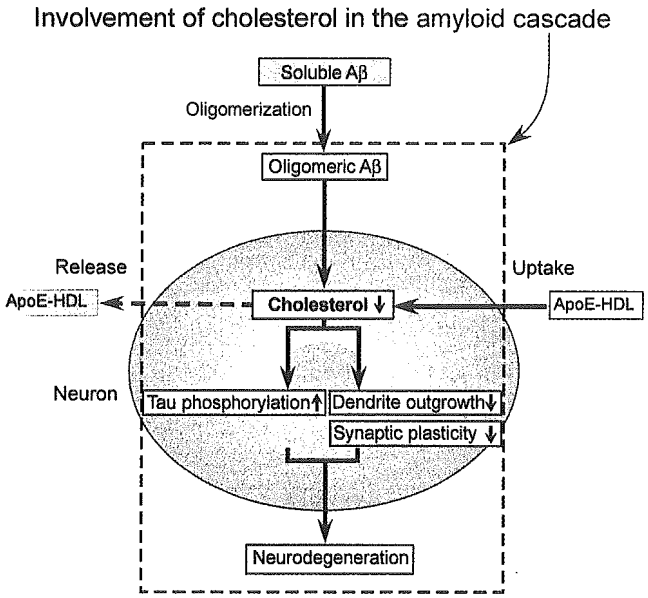

Fig. 1. A hypothetical schema showing a putative role of cholesterol in the amyloid cascade, which is a widely accepted hypothesis on the pathogenesis of AD. Increased levels of cholesterol in cell membranes result in the increased levels of generation and secretion of Aβ, leading to formation of oligomeric and aggregated Aβs. Oligomeric Aβ then reduces the cholesterol level in neurons by promoting cholesterol release from neurons to generate HDL-Aβ complexes (Michikawa et al., 2001) and inhibiting cholesterol synthesis (Gong et al., 2002a). The disruption of cholesterol homeostasis in neuronal membranes caused by oligomeric Aβ may induce AD pathological alterations including enhanced phosphorylation of tau (Fan et al., 2001b; Koudinov and Koudinova, 2001), inhibition of dendrite outgrowth (Fan et al., 2002), impairment of synaptogenesis and synaptic plasticity (Mauch et al., 2001), and neurodegeneration (Michikawa and Yanagisawa, 1999; Koudinov and Koudinova, 2001). ApoE is isoform-dependently involved in this cascade as an HDL generator by supplying cholesterol to neurons (Michikawa et al., 2000; Gong et al., 2002b).

controls (Mulder et al., 1998). In addition, it should be noted that treatment with statins reduces the total cholesterol level but increases HDL cholesterol level, as well as the HDL/LDL and HDL/total cholesterol ratios (Hess et al., 2000; Chong et al., 2002; Gagne et al., 2002). A previous study demonstrated a strong correlation between CSF and serum HDL cholesterol levels, but not between CSF and serum total or LDL cholesterol levels (Fagan et al., 2000). These lines of evidence suggest that the decreased level of HDL in CNS may be associated with a risk of AD development, which is also linked to the decreased level of serum HDL cholesterol, and that statin treatment may help reduce the risk of AD by increasing serum HDL and CSF cholesterol levels. In accordance with this notion, a recent study has shown that in the white matter of brains with AD, the Aβ level increases whereas the cholesterol level decreases (Roher et al., 2002), suggesting the decreased level of cholesterol is associated with neurodegeneration in AD. A recent autopsy-based study has revealed results inconsistent with the above results, however, in that it is not total or LDL cholesterol level but high HDL cholesterol level in plasma that is associated with the increased number of neuritic plaques and neurofibrillary tangles (NFTs) (Launer et al., 2001). Because statin treatment not only reduces total and LDL cholesterol levels, but also increases HDL cholesterol level, further studies are required to better understand how the lipoprotein cholesterol level is associated with the pathogenesis of AD.

ROLE OF CHOLESTEROL IN AMYLOID CASCADE

It was postulated that hyperphosphorylation of tau is a requisite step for the formation of NFTs, one of the major pathological hallmarks in the AD brain. The mechanism underlying accelerated phosphorylation of tau, however, and the subsequent formation of NFTs in the AD brain remain unclear. It is interesting to note that a perturbation of cholesterol metabolism and NFT formation coexist in brains with Niemann-Pick type C disease (Auer et al., 1995; Love et al., 1995; Suzuki et al., 1995); this suggests another possibility of a link between cholesterol and the pathogenesis of AD including tauopathy. Our recent study has shown that tau in the brains of NPC model mice is hyperphosphorylated in a site-specific manner, accompanied by enhanced activity of mitogen-activated kinase (MAPK) (Sawamura et al., 2001). Another line of evidence demonstrated that cholesterol is accumulated in tangle-bearing neurons (Distl et al., 2001). These results may suggest that increased levels of cellular cholesterol promote tau phosphorylation in neurons. It has been found previously, however, that reduced levels of cellular cholesterol promote tau phosphorylation in cultured neurons (Fan et al., 2001b) and in vivo (Koudinov and Koudinova, 2001). In addition, it was found that cholesterol deficiency in lipid rafts (Simons and Ikonen, 1997) is responsible for the induction of tau phosphorylation in NPC1-deficient cells and in cholesterol-deficient neurons (unpublished data), indicating that the state of tau phosphorylation is modulated not by the total cellular cholesterol level but by that of a specific cellular compartment such as lipid rafts, leading to alteration in the intracellular signaling. Interestingly, a deficiency in cellular cholesterol or a deficiency in cholesterol supply to neurons was shown to inhibit dendrite outgrowth (Fan et al., 2002) and synaptogenesis (Koudinov and Koudinova, 2001; Mauch et al., 2001), and to induce neurodegeneration (Michikawa and Yanagisawa, 1999) as well as tauopathy (Fan et al., 2001b; Koudinov and Koudinova, 2001; Sawamura et al., 2001). Although many issues require clarification, particularly regarding various downstream events in the amyloid cascade, these lines of evidence suggest the possible role of cholesterol in this cascade, modulating the processes that induce AD pathologies. In this context, it is noteworthy that oligomeric Aβ affects cellular cholesterol metabolism (Liu et al., 1998; Michikawa et al., 2001) by generating Aβ-lipid particles with a density identical to that of HDL, which cannot be internalized into cells (Michikawa et al., 2001). Importantly, oligomeric but not monomeric Aβ reduces choles-

TABLE I. Lipoprotein-Dependent and apoE-Genotype-Dependent Cholesterol Levels in Serum and CSF of Human Subjects and in Conditioned Medium of Cell Cultures*

Lipoprotein	Cholesterol level	References
Serum total	apoE2 < apoE3 < apoE4	Bouthillier et al., 1983; Davignon et al., 1988; Lehtinen et al., 1995; Braeckman et al., 1996; Frikke-Schmidt et al., 2000
Serum LDL	Control < AD and MCI	Notkola et al., 1998; Evans et al., 2000; Kivipelto et al., 2001
	apoE2 < apoE3 < apoE4	Lehtinen et al., 1995
	Control < AD	NR
Serum HDL	apoE2 > apoE3 > apoE4	Lehtinen et al., 1995; Braeckman et al., 1996; Frikke-Schmidt et al., 2000
	Control > AD	Merched et al., 2000
	Control < AD	Launer et al., 2001
CSF HDL	apoE2 > apoE3 > apoE4	NR
	Control > AD	Mulder et al., 1998
CM HDL	apoE2 > apoE3 > apoE4	Michikawa et al., 2000; Gong et al., 2002b

*CM, conditioned medium of cultured cells; CSF, cerebrospinal fluid; AD, Alzheimer's disease; NR, not reported; MCI, mild cognitive impairment.

terol levels in neurons (Gong et al., 2002a). These findings imply the central role of cholesterol in the amyloid cascade (Fig. 1); that is, the increased level of Aβ oligomers affects cellular cholesterol metabolism, resulting in the reduction in cholesterol levels in neurons, which in turn induces hyperphosphorylation of tau, impairment of synaptic plasticity, and finally, neurodegeneration.

The last question to be addressed is how apoE, which modulates cholesterol metabolism, is involved in this cascade. Our recent studies have shown that the ability of apoE to generate HDL particles is isoform-dependent. The amount of cholesterol released as HDL particles from apoE3-expressing astrocytes was ~2.5-fold greater than that from apoE4-expressing astrocytes with a similar number of each apoE molecule (Gong et al., 2002b). ApoE dependency in the promotion (apoE4) or prevention (apoE3) of AD pathologies can be explained by its isoform-dependent ability (apoE3 > apoE4) in cholesterol release from cultured astrocytes generating HDL-like particles, which could supply cholesterol to neurons (Michikawa et al., 2000; Gong et al., 2002b). Taken all together, it may be possible that the level of oligomeric Aβ that can increase in an aged brain affects brain cholesterol homeostasis, which is compensated for mainly by the apoE isoform-dependent HDL cholesterol supply from astrocytes. The lower ability of apoE4 to generate HDL may result in earlier disruption in cholesterol homeostasis in neurons, leading to tauopathy. In this context, it may also be possible that the decreased HDL level in the CNS linked with a decreased level of serum HDL cholesterol is a risk factor for the development of AD. Statin treatment may contribute to the reduction in the AD prevalence by increasing serum HDL levels, and subsequently, CSF cholesterol levels. Recent studies, however, showing that the cholesterol-lowering effect of statin depends on the presence of functional apoE (Eckert et al., 2001; Wang et al., 2002) may imply an alternative involvement of the apoE genotype in the inhibitory effect of statin on AD development. Further studies are required to characterize cholesterol metabolism in the CSF and brains of human subjects and animals with or without statin treatment, and to clarify the relationship between cholesterol and AD pathogenesis. The different viewpoints presented here might give new insights into the strategy for elucidating the mechanisms underlying the link between cholesterol and AD.

REFERENCES

Auer IA, Schmidt ML, Lee VM, Curry B, Suzuki K, Shin RW, Pentchev PG, Carstea ED, Trojanowski JQ. 1995. Paired helical filament tau (PHFtau) in Niemann-Pick type C disease is similar to PHFtau in Alzheimer's disease. Acta Neuropathol (Berl) 90:547–551.

Borghini I, Barja F, Pometta D, James RW. 1995. Characterization of subpopulations of lipoprotein particles isolated from human cerebrospinal fluid. Biochim Biophys Acta 1255:192–200.

Bouthillier D, Sing CF, Davignon J. 1983. Apolipoprotein E phenotyping with a single gel method: application to the study of informative matings. J Lipid Res 24:1060–1069.

Braeckman L, De Bacquer D, Rosseneu M, De Backer G. 1996. Apolipoprotein E polymorphism in middle-aged Belgian men: phenotype distribution and relation to serum lipids and lipoproteins. Atherosclerosis 120:67–73.

Chong PH, Kezele R, Franklin C. 2002. High-density lipoprotein cholesterol and the role of statins. Circ J 66:1037–1044.

Craig AM, Banker G. 1994. Neuronal polarity. Annu Rev Neurosci 17:267–310.

Davignon J, Gregg RE, Sing CF. 1988. Apolipoprotein E polymorphism and atherosclerosis. Arteriosclerosis 8:1–21.

Distl R, Meske V, Ohm TG. 2001. Tangle-bearing neurons contain more free cholesterol than adjacent tangle-free neurons. Acta Neuropathol (Berl) 101:547–554.

Eckert GP, Kirsch C, Muller WE. 2001. Differential effects of lovastatin treatment on brain cholesterol levels in normal and ApoE-deficient mice. Neuroreport 12:883–887.

Evans RM, Emsley CL, Gao S, Sahota A, Hall KS, Farlow MR, Hendrie H. 2000. Serum cholesterol, APOE genotype, and the risk of Alzheimer's disease: a population-based study of African Americans. Neurology 54: 240–242.